Empirically-Derived Relationship between Growing-Season Average NDVI and Annual ET for White River, Spring, and Snake Valleys, Nevada

PRESENTATION TO THE OFFICE OF THE NEVADA STATE ENGINEER

Prepared by

DRI
Desert Research Institute

and

SOUTHERN NEVADA
WATER AUTHORITY

June 2011

Empirically-Derived Relationship between Growing-Season Average NDVI and Annual ET for White River, Spring, and Snake Valleys, Nevada

Submitted to:
Jason King, P.E., State Engineer
State of Nevada
Department of Conservation & Natural Resources
Division of Water Resources
901 S. Stewart Street, Suite 2002
Carson City, Nevada 89701

Pertaining to:
Groundwater Applications 54003 through 54021 in
Spring Valley
and
Groundwater Applications 53987 through 53992 in
Cave, Dry Lake, and Delamar Valleys

June 2011

Prepared by:
Desert Research Institute
755 East Flamingo Road
Las Vegas, Nevada 89119

and

Southern Nevada Water Authority
Water Resources Division
P.O. Box 99956
Las Vegas, Nevada 89193-9956

_____   6/7/11
Lynn F. Fenstermaker, Ph.D., Remote Sensing Research Professor,   Date
Desert Research Institute

_____   6·14·11
Andrew G. Burns, Water Resources Division Manager   Date
Southern Nevada Water Authority

CONTENTS

CONTENTS (CONTINUED)

FIGURES

FIGURES (CONTINUED)

TABLES

This Page Left Intentionally Blank

ACRONYMS

BARCASS	Basin and Range Carbonate Aquifer System Study
CI	confidence interval
DEM	digital elevation model
DRI	Desert Research Institute
EBR	energy balance ratio
EC	eddy covariance
ENVI	ENvironment for Visualizing Images
EROS	Earth Resources Observation and Science
ET	evapotranspiration
ET_{ref}	reference ET
EVI	enhanced vegetation index
MODIS	MODerate Resolution Imaging Spectroradiometer
MSAVI	modified soil adjusted vegetation index
NAD83	North American Datum of 1983
NDVI	normalized difference vegetation index
QA	quality assurance
QC	quality control
ROI	region-of-interest
SEBAL	Surface Energy Balance Algorithm for Land
SNWA	Southern Nevada Water Authority
SP	single pixel
SWReGAP	Southwest Regional GAP Analysis Project
TM	Thematic Mapper
UNLV	University of Nevada, Las Vegas
USGS	U.S. Geological Survey
UTM	Universal Transverse Mercator
VI	vegetation index

ABBREVIATIONS

af	acre-feet
ags	above ground surface
amsl	above mean sea level
bgs	below ground surface
ft	foot

ABBREVIATIONS (CONTINUED)

Hz	hertz
in.	inch
m	meter
m^2	square meter
min	minute
MJ	megajoules
mm	millimeter
μm	micrometer
nm	nanometer
yr	year

1.0 INTRODUCTION

This report documents the acquisition, processing, and analysis of micrometeorological data and satellite imagery collected as part of a multi-year collaborative investigation completed by the University of Nevada, Las Vegas (UNLV), Desert Research Institute (DRI), and the Southern Nevada Water Authority (SNWA) to evaluate and quantify evapotranspiration (ET) within groundwater discharge areas of White River, Spring, and Snake Valleys, Nevada. The locations of these valleys are presented in Figure 1-1, and are hereinafter referred to collectively as the basins of interest.

1.1 Background

ET is the principle mechanism by which groundwater is discharged, and also represents the largest component of the groundwater budget in the basins of interest. This is of particular interest to SNWA because SNWA holds applications for groundwater permits in Spring and Snake Valleys, and in hydrographic areas of the White River Flow System in which White River Valley resides. Thus in 2004, SNWA initiated a study with UNLV to estimate ET within Spring and White River Valleys. The study was expanded in 2007 to include Snake Valley (Devitt et al., 2008, 2010). By the end of 2007, responsibility for the maintenance of these sites and the data acquisition and processing was assumed by SNWA, who has since continued these efforts to the present. Also in 2007, SNWA expanded the scope of the investigation by initiating a study with DRI for additional ET monitoring in Spring Valley that encompassed a one-year period from April 2007 to April 2008 (Arnone et al., 2008). SNWA provided additional funding at the end of this one-year period to extend the data collection through October 2009. SNWA's primary objective for initiating these studies was to refine previous estimates of annual ET rates using newer methodologies to support the development of groundwater budgets in the basins of interest. Both studies used Eddy Covariance (EC) systems to measure ET rates for specific plant communities, and remote sensing methods to scale those rates to estimate annual ET for the entire groundwater discharge areas. EC stations were eventually established in all three valleys for the UNLV study, and included one in White River Valley, three in Spring Valley and two in Snake Valley. The DRI study was performed for Spring Valley only and utilized four new EC stations in that valley. Figure 1-1 depicts the ET-measurement sites within the groundwater discharge areas of the basins of interest. These studies are discussed in greater detail in the Section 2.0.

1.2 Purpose and Scope

This document reports on an on-going effort to accurately estimate annual ET in Spring and White River Valleys in east central Nevada. The primary objective has been the development of an empirical relationship between growing-season average NDVI and annual ET using satellite imagery and EC-station data collected at sites located within the groundwater discharge areas of Spring, Snake and White River Valleys. These data were collected during the period 2006 through 2010, and were
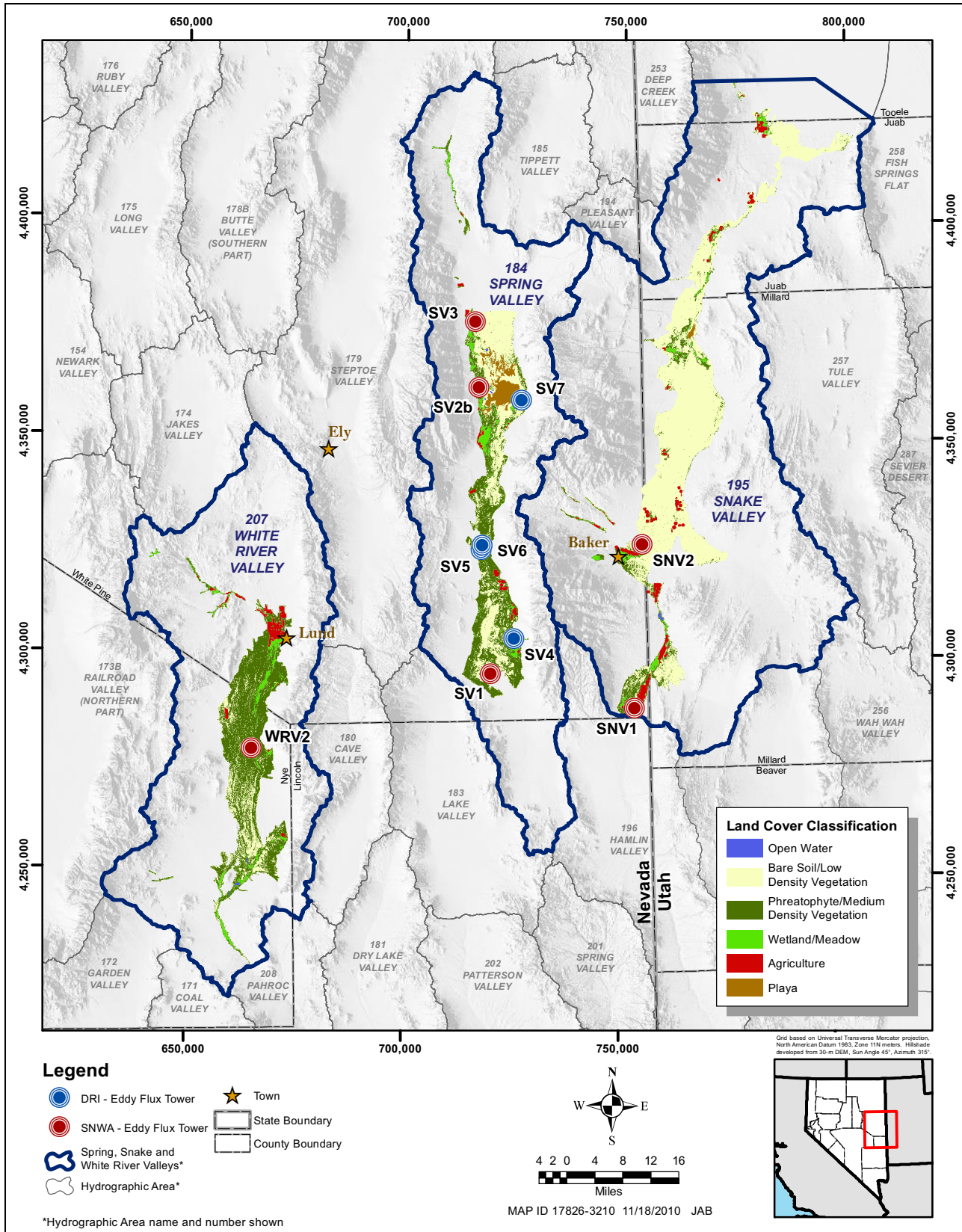
Figure 1-1
Locations of UNLV, DRI, and SNWA ET-Measurement Sites

processed and analyzed using linear regression to derive the empirical relationship. This effort therefore reanalyzed data acquired by Devitt et al. (2008, 2010) and Arnone et al. (2008), as well as new data acquired during the period 2008 through 2010. Several data points were reserved from the regression analysis to perform an independent assessment of the accuracy of the regression-model predictions. The regression model can then be applied to growing-season average NDVI grids to estimate basin-scale annual ET with a quantified accuracy for both Spring and White River Valleys. A combination of methods from the prior Devitt et al. (2008) and the Arnone et al. (2008) studies was used for the analysis of the five-year time period reported in this document. These studies and the specific methods applied in this analysis are discussed in detail in Section 2.0.

This Page Left Intentionally Blank

2.0 TECHNICAL APPROACH

2.1   Background

Estimation of ET over large spatial and temporal scales is dependent on remote sensing data methods because direct measurements are limited to station-based, lysimeter or finer scale (e.g., sap flow and leaf-chamber) water-flux measurements. Over the past several decades numerous researchers have investigated remote sensing techniques to estimate ET for large spatial areas; see reviews by Moran and Jackson (1991); Courault et al. (2005); and Glenn et al. (2007). The use of remote sensing makes it possible to extend field-based measurements within a specific plant community across a larger spatial distribution of the same or similar plant community within the broader landscape.

While several methods have been developed for estimating ET using remote sensing data, most of these could be categorized into two groups: (1) empirical or statistical approaches based on regression relationships between ground-based ET measurements and vegetation indices (VI); and (2) physical models based on the surface energy balance equation, which include models such as the Surface Energy Balance Algorithm for Land (SEBAL; Bastiaanssen et al., 1998a and b) and Mapping Evapotranspiration with Internalized Calibration (METRIC; Allen et al., 2005), which was derived from SEBAL. One of the critical limitations of empirical methods in comparison to physical models is the fact that empirical approaches do not provide any information on surface flux components (sensible and latent heat) that drive ET and thus are not useful for climate modeling purposes (Glenn et al., 2007). However, when only an estimate of ET is desired an empirical relationship between ET and VI values provides a means to estimate total ET for a desired time period without interpolating between satellite overpass dates. Physical models based on energy balance approaches are temporally limited in that these methods can only assess instantaneous to 24-hour energy fluxes and resulting ET. Determination of ET beyond a 24-hour period requires interpolation between satellite acquisition dates (see Glenn et al., 2007 for an assessment of the method). Relevant investigations involving the application of these methods are described in the following section.

2.2   Review of Relevant Investigations

As early as 1988, Running and Nemani found good regression relationships between ET and a VI derived from remote sensing data, which has continued into the present (Nagler et al., 2007). A regression relationship between annual ET and average growing season VI values overcomes the autocorrelation between ET and VIs that occurs at single points-in-time due to similar seasonal trends (Szilagyi 2000, 2002).

A number of remote sensing studies have focused on ET estimation in riparian or cropland areas for irrigation scheduling and water rights issues (Allen et al., 2005, 2007; Nagler et al., 2005), however, there are only a few remote sensing studies that have examined ET in semi-arid shrubland areas

(i.e., Kustas et al., 1994; Tuya et al., 2005; Nagler et al., 2007) where vegetation canopies are sparse and water is limited. This is particularly true for the Great Basin of east central Nevada. Nichols (2000) developed an equation to estimate ET for phreatophytic areas based on a relationship between plant cover/groundwater depth and Bowen Ratio and other ET measurements at Owens Valley California and four locations in Nevada (none of which coincides with the valleys examined in this report). Because these estimates were based on point measurements and did not use any spatially continuous data, the representativeness of the point measurements to the broader landscape is questionable. The most relevant investigations pertaining to the basins of interest include the aforementioned UNLV and DRI studies, and a U.S. Geological Survey (USGS) study completed as part of the Basin and Range Carbonate Aquifer System Study (BARCASS). These three studies are described in greater detail in the following subsections.

2.2.1   UNLV ET Study

Devitt et al. (2008; 2010) examined two empirical approaches to estimate total annual ET within the phreatophytic area of the three valleys. The first approach (single date) developed a regression relationship between daily, single-pixel, normalized difference vegetation index values (NDVI; Rouse et al., 1974) for each Landsat image date and daily ET values. The daily basin ET estimates were then plotted as a function of time and the area under the response curve was estimated using integration to derive total annual ET for each basin. The primary issue with this approach was the likely over-estimation of ET because only ET measurements for relatively cloud-free dates were used for the analysis. Satellite images with a lot of cloud cover cannot be used for this type of data analysis because the clouds obscure all ground features beneath them. However, when cloud cover is present incoming solar radiation is typically diminished resulting in lower ET rates. Therefore the application of a spline function between cloud-free image dates does not account for decreased ET rates that occur with increasing cloud cover and other varying environmental factors. The second approach developed a regression relationship between average growing season NDVI values and annual ET. Because average NDVI values were regressed with annual ET, this approach accounted for varying rates of ET that occurred during the year and thus had a higher likelihood of producing accurate ET estimates. Devitt et al. (2008) used the regression equation to calculate an image containing pixels with ET values. These ET values were summed for each valley to produce an estimate of total annual ET.

2.2.2   DRI ET Study

Arnone et al. (2008) also regressed average growing season NDVI with annual ET and also examined the relationship between the Enhanced Vegetation Index (EVI; Huete et al., 2002; Nagler et al., 2007) and annual ET. Recent publications by Nagler et al. (2005; 2007), had reported a strong relationship between EVI and ET and hence Arnone et al. (2008) wanted to compare results between the NDVI and EVI. The Arnone et al. (2008) study did not find any significant differences between the NDVI and EVI relationships with ET. EVI was originally developed for the MODIS (MODerate resolution Imaging Spectroradiometer) satellite sensor; therefore, the bandwidths used to generate EVI from MODIS are different than the bandwidths of the Landsat satellite sensors and hence may not provide the same results.

Arnone et al. (2008) methods also varied from Devitt et al. (2008) by not using a single pixel average NDVI or EVI value to regress with annual ET. Instead, Arnone et al. (2008) calculated the boundaries of annual footprints for each EC station and derived an average NDVI and EVI value for all pixels falling within the annual footprint boundary and used this value to regress with annual ET. The ET measured by an EC station encompasses an area that changes based on wind speed and direction, therefore, the DRI team believed that an average NDVI or EVI value within the annual station footprint would more accurately represent the vegetation and land surface being measured by that station. Arnone et al. (2008) also looked at single versus two regression relationships for areas that are and are not water limited, e.g., wetland meadows and irrigated agriculture versus shrubland areas where a lack of near-surface water limits ET. One relationship (Eq. 1) was based on regression between annual ET and average NDVI (and EVI) values for all station sites. The second relationship (Eq. 2) was a simple ratio between annual ET and the average NDVI (and EVI) value for the single irrigated agricultural station site, and the third relationship (Eq. 3) was between annual ET and average NDVI (and EVI) values for the shrubland sites. Combinations of these regression relationships (Approach 1: Eq. 1 for all pixels; Approach 2: Eq. 1 for shrubland pixels and Eq. 2 for irrigated agriculture pixels; and Approach 3: Eq. 3 for shrubland pixels and Eq. 2 for irrigated agriculture pixels) were used to calculate ET values for each image pixel (an ET image). The individual ET values were summed to produce an estimate of total annual ET for Spring Valley.

Actual measurements of annual ET were compared to predicted annual ET resulting from application of the regression equations to the average growing season NDVI and EVI images. Residuals varied from an under-prediction of 74 mm for the irrigated agriculture site to an over-prediction of 26 mm for one of the dense shrub sites (SV6). The percent error was relatively small, ranging from 4.29 percent (EVI, Approach 1) to 7.56 percent (NDVI, Approach 3), regardless of VI and regression equations used (Eqs. 1 through 3). However, it must be noted that a valid accuracy assessment with independent data (i.e., data not used in the regression calculation) was not performed and therefore the percent errors reported indicate a best case accuracy.

2.2.3   USGS ET Study

The USGS initiated an ET study in the same valleys during a 2005-2006 period (Welch et al., 2007 with additional details on ET measurements and remote sensing analyses in Moreo et al., 2007 and Smith et al., 2007, respectively). The USGS study encompassed six sites where EC stations were deployed: two in White River Valley, three in Spring Valley and one in Snake Valley.

The USGS study used a different approach than the UNLV and DRI studies by developing ET classes for empirical analysis with EC data (EC data reported in Moreo et al., 2007) using a single date Landsat multiscene image for White River Valley (July 3, 2005) and another single date Landsat multiscene image for Spring and Snake Valleys (July 12, 2005; Smith et al., 2007). Multiscene is a term used to define several adjacent Landsat scenes acquired within the same satellite path on the same date. USGS acquired three adjacent scenes within each of the two multiscenes. The ET classes Smith et al. (2007) developed included the Southwest Regional GAP Analysis Project (SWReGAP) marshland, dry playa and open water bodies ET classes. Other ET classes were developed using a modified soil adjusted vegetation index (MSAVI) for phreatophytic shrubs and grasses, and a tasseled cap transformation to map moist bare soil. The end result was the development of an ET class image that encompassed open water, marshland, dry playa, irrigated cropland, shrubland, grassland,

meadow, moist bare soil and xerophyte. An average annual ET rate was estimated by multiplying the annual ET by the area of the ET class within which the EC stations were located. A range in annual ET rates was determined based on the ET measured at EC sites of similar vegetation composition. These ranges were then applied to the ET class images for each valley, applying the highest estimated annual ET rate to pixels with the highest MSAVI values and the lowest estimated annual ET rate to pixels with the lowest MSAVI values.

2.3   Accuracy of ET-Estimation Methods Applied in the Basins of Interest

Prior to analyzing five years of data for this report, a series of assessments were performed by DRI and SNWA to ensure that the best methods would be employed. This describes the analyses that were performed to assess the accuracy of the three studies discussed in the previous sections, (i.e., USGS as reported in Moreo et al., 2007; Smith et al., 2007; and Welch et al., 2007; UNLV as reported in Devitt et al., 2008, 2010; and DRI as reported in Arnone et al., 2008).

Smith et al. (2007) performed an accuracy assessment of the ET class map (28 points in Snake Valley and 38 in Spring Valley) using field methods adapted from the SWReGAP (Field Methodologies and Training Manual for Nevada Field Crews, Sajwaj, 2003). The assessment tested the accuracy of the image classification and found overall user accuracies ranging from 25 percent for marshland to 100 percent for irrigated cropland; shrubland areas had accuracies ranging from 53 to 94 percent with the dense shrub covered areas having the least accuracy and the sparsest shrub cover areas having the highest accuracy. While knowledge of the classification accuracy is critical it does not provide an assessment on the accuracy of the final ET calculation. Zhu et al. (2007) performed an uncertainty analysis of the USGS ET predictions and reported uncertainties of approximately ±19,000 to ±20,000 af, which equates to a potential percent error of 24 percent. However, the uncertainty analysis did not use independent data to assess error and thus the actual percent errors may be larger or smaller than the uncertainty values reported. Because it was not possible to directly access the USGS datasets that were used to estimate total annual ET within each valley, further accuracy assessment analysis was not possible and therefore this methodology was not adopted for the five-year data analysis reported later in this document.

Both of the UNLV and DRI efforts reported that an empirical approach encompassing the entire year provided more robust relationships for scaling to the basin level than an examination of individual dates associated with the availability of satellite remote sensing data. However, an assessment of the accuracy of these relationships was not explored with independent data and further assessment of methodologies was not performed in these studies. An external peer review was conducted for each study by Dr. Pam Nagler of the USGS Sonoran Desert Research Station (Nagler, pers. comm., 2009). Dr. Nagler has experience measuring ET and using MODIS data to develop empirical relationships between ET and VIs. The review focused on the technical approach, overall soundness of the methods, and reliability of the conclusions. Dr. Nagler found both studies to be well-conducted and produce reliable estimates of ET, however, she noted that the Arnone et al. (2008) study results were based on limited data. The most applicable and sound approach for estimating ET on a basin-wide scale, however, likely is a combination of the two approaches and hence the efforts/tasks described in this report build upon those efforts with enhanced methods for estimating annual basin ET using an empirical remote sensing approach.

To assess the accuracy of the Devitt et al. (2008) and Arnone et al. (2008) empirical approaches to total annual ET estimation, DRI and SNWA undertook an effort to quantify both the "fit" of the regression equations and an accuracy assessment using independent data. The regression equation fit is an assessment of how closely the regression equation calculates an estimated annual ET value for the same data used to generate the regression equation, which should be a reasonably close match. The accuracy assessment portion of the effort used annual ET data that had not been used in the regression analysis and thus could serve as an independent measure of the predicted annual ET accuracy. Because the DRI ET data were not used by Devitt et al. (2008) and UNLV data were not used for the Arnone et al. (2008) study, the DRI data served as the independent data for accuracy assessment of the Devitt et al. (2008) average NDVI to annual ET approach and the UNLV/SNWA data served as independent data for accuracy assessment of the six Arnone et al. (2008) approaches, (i.e., three approaches each for the average NDVI and average EVI data).

The Devitt et al. (2008) NDVI to ET empirical relationship was derived from regression analysis of the ET-measurement site single pixel NDVI values extracted from average growing season NDVI images for 2006 and 2007 and the total annual ET measured by the UNLV and BARCASS EC stations for the same two years (Note: Because the Devitt study ended in September 2007, the annual ET value was extrapolated to the end of the calendar year). This approach will be referred to as the NDVI single pixel (NDVI-SP) approach. The Arnone et al. (2008) VI to ET empirical relationships were derived from regression analysis of the measurement-site footprint average NDVI and EVI values extracted from average growing season NDVI and EVI images and total annual ET measured by the four DRI EC stations located in Spring Valley. These approaches are referred to as the NDVI and EVI footprint approaches, NDVI-Fx and EVI-Fx, where x is the number 1, 2 or 3 and refers to the three approaches (where 1 = regression equation 1, 2 = regression equations 1 and 2, and 3 = regression equations 2 and 3; see previous description in Section 2.2.2) developed by Arnone et al. (2008) from average NDVI and EVI values within each site's annual footprint boundary.

The predicted annual ET values for each site were compared to annual ET measured by the EC stations. Figure 2-1 depicts the correspondence between predicted and measured annual ET for the Devitt et al. (2008) approach and the Arnone et al. (2008) approaches with data that was used to develop the regression equations. The graphs show that while there is not a 1:1 correspondence (black line) between predicted and measured ET, the values are close for all seven approaches. The NDVI-F3, EVI-F2 and EVI-F3 generally produced predicted ET values that were closest to the 1:1 line, (e.g., most similar to measured ET values).

To provide a quantitative assessment of the regression fit as well as an accuracy assessment, the percent errors for the seven Spring Valley measurement sites were calculated. The residuals for both the regression fit and accuracy assessment were calculated and then divided by the total measured ET data to produce a percent error, presented in Figure 2-2. The results of this effort revealed that the footprint approaches performed better than the single pixel approach (both regression fit and accuracy assessment). Among the footprint approaches, the EVI approaches had slightly smaller percent errors for the regression fit but had larger percent errors for the accuracy assessment (black bars). Figure 2-2 also indicates that the use of two equations (-F2 and -F3) to predict ET for shrub and irrigated agricultural areas produces slightly more accurate results.
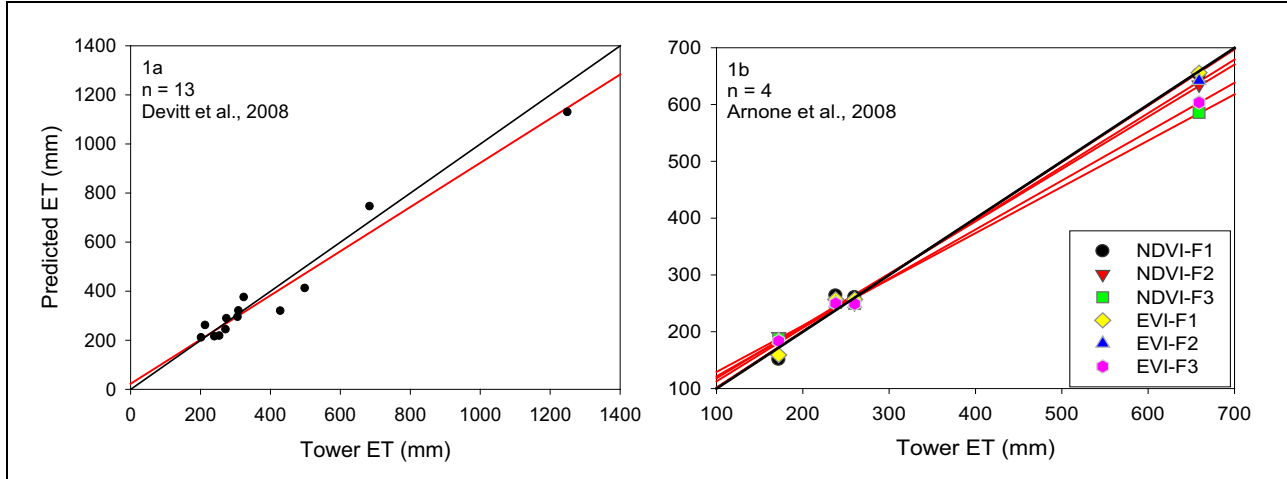
Above is a depiction of the "fit" (e.g., regression relationship) between the annual tower and predicted ET for the Devitt et al. (2008) single-pixel empirical relationship, NDVI-SP (1a; r² = 0.961, n = 13) and the Arnone et al. (2008) footprint empirical relationships (1b; r² = 0.988 to 0.997, n = 4). The data are the same as that used to generate the regression relationships in the Devitt et al. (2008) and Arnone et al. (2008) reports. Notes: a black 1:1 diagonal line (e.g., no difference between predicted and tower ET) is graphed to provide a reference for the regression lines graphed in red; and the scale of the y-axis for the two graphs differ because of the significantly higher annual ET value at the irrigated Spring Valley 2b agricultural tower location, graph 1a.

Figure 2-1
Devitt et al. (2008) and Arnone et al. (2008) Regression Relationships
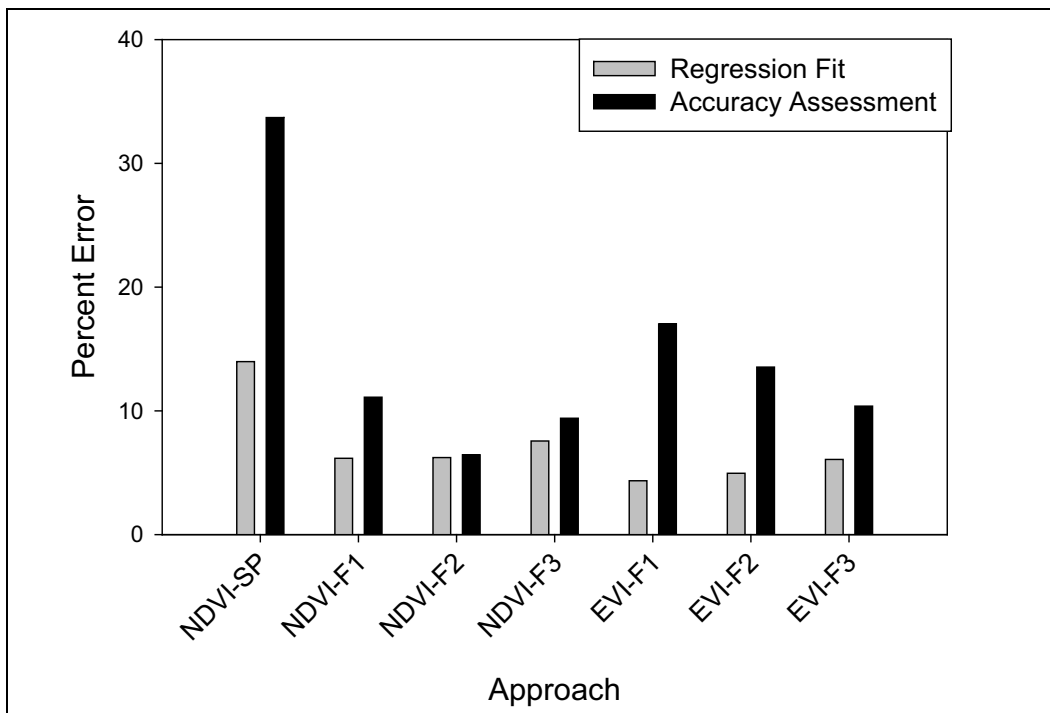
The percent error between predicted and measured ET are graphed for each of the seven empirical approaches examined collectively by Devitt et al. (2008) - NDVI-SP and Arnone et al. (2008) - NDVI-F1, NDVI-F2, NDVI-F3, EVI-F1, EVI-F2 and EVI-F3. The gray bars depict the percent error of the regression fit for the measured data used to generate each empirical approach. The black bars are the percent error for the independent station data used in the accuracy assessment.

Figure 2-2
Percent Error of Devitt et al. (2008) and
Arnone et al. (2008) Regression Relationships

An examination of errors reported in the literature indicates that the errors found in the Devitt et al. (2008) and Arnone et al. (2008) approaches are either similar to or better than other published results. Most of the research reported in the literature examines ET on a daily basis and as such the errors reported are daily errors, which likely will not scale directly to an annual error due to limited representation of weather variability throughout the year. For example, Gao and Long (2008) reported daily errors ranging from 3.18 to 5.01 mm or 2.2 to 5.6 percent with the best remote sensing ET Model tested, e.g., Parallel Two-Source Energy Balance (P-TSEB), and 9.11 to 26.56 percent error for the other two models tested, e.g., SEBAL and the Surface Energy Balance System (SEBS), both of which are one source energy balance models. Groeneveld et al. (2007) reported errors as large as 151.5 mm/year for estimation of ET at a single site using a scaled NDVI equation that incorporated precipitation. Their largest average error was 45 mm/year or a 12 percent error. Nagler et al. (2005) reported potential errors of ±25 percent using a scaled EVI empirical relationship that included air temperature as a variable to estimate annual ET. All of the Devitt et al. (2008) and Arnone et al. (2008) approaches predict ET with a similar or slightly better percent error, (e.g., from 6 percent error for NDVI-F2 to 34 percent error for NDVI-SP as depicted in Figure 2-2).

2.4   Selected Method

Based on the regression analyses and accuracy assessment results summarized in the preceding section for the Devitt et al. (2008) and Arnone et al. (2008) empirical relationships, it was determined that similar footprint-based regression methods would be employed for this effort using the NDVI, which yielded a slightly higher accuracy than the EVI approaches. However, instead of using an average value within the annual footprint boundary, where every pixel has an equal weighting, it was determined that a footprint-weighted average value would provide a more realistic average NDVI value. This decision was based on additional work performed by DRI and SNWA examining the accuracies of a single pixel versus average values within annual footprint boundaries or footprint-weighted average annual values. By weighting the pixels based on wind speed and wind direction measurements, it is thus possible to account for the areas around the tower that provide a larger contribution to the ET measured by the EC station. The results of the DRI and SNWA assessment of single pixel versus footprint approaches revealed a best fit and improved accuracy with the footprint-weighted average annual values (i.e., 22 percent improvement in percent error versus average within the footprint boundary).

The primary objectives of the effort reported here were to (1) report EC station data and annual ET measurements; (2) develop average growing-season NDVI images (AvgNDVI) for each year; (3) calculate EC-station annual footprints for each measurement site and year; (4) apply the footprints to the AvgNDVI images to produce a weighted-average NDVI value for regression analysis; (5) perform regression analysis between weighted-average NDVI values and annual ET; and (6) perform an independent accuracy assessment of regression-model predictions using data points reserved from the regression analysis.

2.4.1   Data Requirements and Sources

The data required to complete the analysis described in this report included annual ET data measured by EC stations located in the basins of interest, Landsat Thematic Mapper (TM) 5 scenes, and

meteorological data from ET-measurement sites used to calculate annual station footprints. The list below summarizes these data:

- EC-station and meteorological data collected at UNLV, DRI, and SNWA ET-measurement sites. These data were required to derive annual ET measurements and footprint-weighted growing season NDVI values, and are presented in Section 3.0 with more detailed information presented in Shanahan et al. (2011).

- Landsat Thematic Mapper 5 scenes acquired for Spring, Snake and White River Valleys for each of five years between 2006 and 2010. Only scenes during the growing season with 30 percent or less cloud cover were acquired.

- Annual footprints with weighted counts calculated for each station location and year using EC-station and meteorological data collected at the ET-measurement sites.

- Values of annual ET and footprint-weighted growing-season average NDVI for ET measurement sites.

3.0 ET-STATION DATA ACQUISITION AND PROCESSING

3.1 ET-Station Data

Micrometeorological stations were installed at a network of ET-measurement sites within the groundwater discharge areas of White River, Spring and Snake Valleys. The stations were installed at sites representative of various phreatophytic vegetation assemblages and densities, and were instrumented with EC sensors to measure energy fluxes, specifically ET. The EC method was selected over other methods of measuring ground-based ET such as weighing lysimeters or bowen-ratio towers because it is the most direct and defensible way to measure fluxes of heat, water vapor and gas concentrations and momentum between the atmosphere and biosphere (Burba and Anderson, 2010). The measurement sites were selected to ensure each had a sufficient and representative area contributing to the measured flux (i.e., footprint).

The following sections provide summary descriptions of the energy balance and the EC method and data collected at the UNLV, DRI, and SNWA ET-measurement sites in Spring, White River, and Snake Valleys, including physical descriptions of sites and station instrumentation, data collection, processing, and evaluation methods, and annual ET measurements. More detailed information regarding data collection at these sites is presented in Shanahan et al. (2011).

3.1.1 Energy Budget and EC Method of Measuring ET

The sun provides radiant energy to the earth's surface and drives processes of energy exchange between the earth's surface and the atmosphere, including the process of ET. The incoming radiant energy from the sun is commonly referred to as net radiation which is the difference between incoming and outgoing long- and short-wave radiation. Net radiation represents available radiant energy at the earth's surface and therefore is balanced by three key flux terms: latent heat flux which is the energy absorbed or released when water is converted between liquid and gas phases; sensible heat flux which is the heat energy that can be sensed as a positive or negative temperature change; and soil heat flux which is the vertical conductance of heat into or out of the ground. The transfer of this energy is illustrated by the schematic presented in Figure 3-1, and is expressed by the energy budget equation as defined by Brustaert (1982, p. 2):
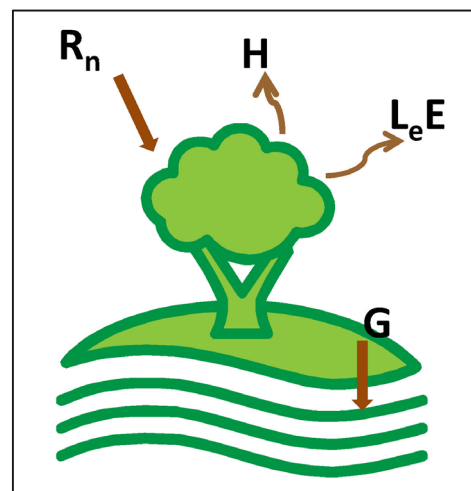
**Figure 3-1
Simplified Schematic of
the Energy Budget**

$$R_n = L_eE + H + G \qquad \text{(Eq. 3-1)}$$

where,

R_n = Net Radiation [watts per square meter]
G = Soil heat flux [watts per square meter]
H = Sensible heat flux [watts per square meter]
L_eE = Latent heat flux [watts per square meter]

The latent heat flux is the energy used to drive the ET process by changing solid or liquid phases of water into vapor, where L_e is the latent heat of evaporation and E is the rate of evaporation. The latent heat flux can be computed using Equation 3-1 and known values of the remaining parameters, or can be measured directly using the EC method.

The EC method has been widely used to measure latent heat fluxes because of its ability to resolve vertical flux densities of water vapor between the atmosphere and biosphere that are directly proportional to the average covariance between the vertical wind velocity and scalar water concentrations (Baldocchi et al., 1996; Massman, 2000; Lee et al., 2004; Wohlfahrt et al., 2008). The method is a sophisticated approach that uses state-of-the-art sensors to measure turbulent fluxes, or eddies, that transport parcels of air upward and downward at certain speeds while moving across the landscape (atmospheric eddy transport). Each eddy has specific heat, water vapor and gas concentration properties. By measuring these properties simultaneously with the speed of vertical air movement, the amount of upward and downward fluxes of heat, water vapor and gas concentration can be determined (Burba and Anderson, 2010).

The latent heat flux measured by the EC sensors can be converted to a rate of evaporation by dividing the measured values by the latent heat of evaporation (L_e), described as L_v in Oke (1987), times the density of water (ρ_w) using Equation 3-2 (based on Oke, 1987, p. 398-399). The rate of evaporation is expressed in units of millimeters per 30-min measurement interval.

$$E = 0.0018LE/(L_e \times \rho_w) \times 1000 \qquad \text{(Eq. 3-2)}$$

where,

E = Rate of evaporation [millimeters per 30-min measurement interval]
LE = Measured latent heat flux [watts per square meter]
ρ_w = Density of water [kilogram per cubic meter]
L_e = Latent heat of evaporation [MegaJoules per kilogram]

and 0.0018 is a unit conversion factor used to convert average 30-min LE values from [W/m^2] to [MJ/m^2 per 30-min period]. Values for ρ_w and L_e were computed as a function of the sonic temperature, T_s, measured by the EC three-dimensional sonic anemometer sensor. The empirical relationships for ρ_w and L_e as a function of temperature are provided in Shanahan et al. (2011, p. 2-3).

3.1.2   ET Measurement-Site Descriptions and Station Instrumentation

A total of ten ET-measurement sites were selected for monitoring within the groundwater discharge areas of White River, Spring, and Snake Valleys. The site locations were selected to represent a range of uniform-composition phreatophytic vegetation for defined land-cover classifications, and to ensure representative measurement of the energy fluxes/atmospheric conditions driving the ET process by locating the site within a sufficiently large area of each class.

The sites were monitored during the period 2006 through 2010 by UNLV, DRI, and SNWA. Some of these sites were monitored prior to 2006, but these data are not included in this analysis because the stations were rotated among several sites, thus yielding incomplete annual data sets. At each site, an EC station and meteorological station was installed. The locations of the measurement-sites are presented in Figure 1-1, and a description of each is provided in Table 3-1.

The EC stations were equipped with high frequency sensors required for the EC method and additional meteorological and ancillary sensors for measuring energy budget and reference ET parameters, physical properties of the soil, and precipitation. The sensors were mounted at heights and depths as required for the EC method and recommended by manufacturer guidelines. Meteorological stations were equipped with sensors and instruments to measure parameters needed to derive reference ET using the Penman-Monteith equation. Some of the same sensors installed as part of the EC station were installed with the meteorological station to collect data for comparison and validation purposes.

All sensors were calibrated routinely per the manufacturer's recommended schedule. The measurement protocols, sensor installation, maintenance, and calibrations were based on the sensor manufacturer, Fluxnet-Canada (2003), and Ameriflux (Munger and Loescher, 2006) guidelines. Table 3-2 lists the measurement type, sensor type, and sensor placement for the SNWA EC stations, meteorological stations, and monitor wells. Figure 3-2a and b illustrate the typical deployment of the EC sensors and meteorological sensors, respectively.

3.1.3   Data Collection, Processing, and Reduction

High resolution 10Hz measurement data were collected and processed real-time by the data logger routines to yield 30-min averages. These raw data were downloaded every 4 to 6 weeks and processed using rigorous screening procedures to yield mean 30-min flux values. The data processing workflow and quality assurance/quality control (QA/QC) measures applied to the raw data are depicted in Figure 3-3. Data for individual parameters were collected and processed according to the manufacturer, Fluxnet-Canada (2003) and Ameriflux guidelines (Munger and Loescher, 2006). All data were post-processed using the EdiRe software package (EdiRe, 1999) to yield corrected flux values. These values were then checked using eleven QA/QC tests to verify optimal sensor and data logger performance, adequately developed turbulence, and statistically stable fluxes. Supplemental data collected from the meteorological stations, monitor wells and soil sensors were used to verify the timing and magnitude of corrected flux measurements. The flux calculations, corrections, and applied QA/QC tests used in the post-processing were collaboratively derived among UNLV, DRI and SNWA and are consistent with Lee et al. (2004), Xu (2004), Ameriflux guidelines (Munger and Loescher, 2006), and Burba and Anderson (2010).

Table 3-1
ET-Measurement Site Descriptions
(Page 1 of 2)
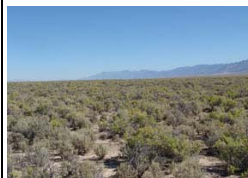
| Site Name | Location[a] | | Altitude (ft amsl) | Installation Date | Site Description[b] | Photograph |
	UTM Northing	UTM Easting				
WRV2						
Met Station	4,277,368	664,984	5,311	Aug 2004	55% cover; predominantly sagebrush and greasewood with minor amounts of shadscale	
EC Station	4,277,445	665,017	5,308	Aug 2004		
Well	4,277,374	665,077	5,314	May 2006		
SV1						
Met Station	4,294,921	720,012	5,780	Sept 2004	27% cover; predominantly sagebrush with rabbitbrush and greasewood; shadscale and buckwheat also present	
EC Station	4,294,919	719,920	5,780	Sept 2004		
Well	4,294,854	720,049	5,783	May 2006		
SV2b						
Met Station	4,360,824	716,789	5,594	March 2007	irrigated pasture/grassland; 100% cover of perennial grasses.	
EC Station	4,360,829	716,743	5,595	March 2007		
Well	4,360,825	716,792	5595	October 2008		
SV3						
Met Station	4,375,833	715,822	5,614	May 2005	32% cover; predominantly greasewood and rabbitbrush; shadscale and pickleweed also present	
EC Station	4,375,912	715,857	5,615	May 2005		
Well	4,375,797	715,452	5,628	May 2007		
SV4						
Met Station	4,303,124	725,313	5,816	April 2007	Irrigated pasture/grassland; 100% cover of perennial grasses	
EC Station	4,303,125	725,311	5,816	April 2007		
Well	4,303,127	725,316	5,817	May 2007		
SV5						
Met Station	4,323,394	717,655	5,774	April 2007	87% cover; mixed stand of greasewood, sagebrush, and rabbitbrush	
EC Station	4,323,395	717,653	5,774	April 2007		
Well	4,323,360	717,660	5,775	May 2007		

Table 3-1
ET-Measurement Site Descriptions
(Page 2 of 2)

| Site Name | Location[a] | | Altitude (ft amsl) | Installation Date | Site Description[b] | Photograph |
	UTM Northing	UTM Easting				
SV6						
Met Station	4,324,556	717,827	5,760	April 2007	76% cover; mixed stand of greasewood, sagebrush, and rabbitbrush.	
EC Station	4,324,555	717,824	5,760	April 2007		
Well	4,324,577	717,853	5,759	May 2007		
SV7						
Met Station	4,357,985	726,577	5,555	April 2007	19% cover; homogenous stand of greasewood	
EC Station	4,357,985	726,575	5,555	April 2007		
Well	4,357,989	726,577	5,555	May 2007		
SNV1						
Met Station	4,287,287	753,159	5,528	April 2007	62% cover; predominantly greasewood with minor amounts of shadscale and sagebrush	
EC Station	4,287,266	753,182	5,528	April 2007		
Well	4,287,317	753,331	5,531	May 2007		
SNV2						
Met Station	4,325,082	754,576	5,133	April 2007	13% cover; mixed community of rabbitbrush, greasewood, sagebrush, and shadscale	
EC Station	4,325,090	754,601	5,132	April 2007		
Well	4,325,458	754,502	5,138	May 2007		

[a]Universal Transverse Mercator (UTM), North American Datum of 1983 (NAD83), Zone 11.
[b]Percent cover estimates from Devitt et al. (2008) and Arnone et al. (2008)

A subset of the data failed the QA/QC tests due to periodic equipment failure and/or inclement weather that affected the measurement of the various parameters. These data were removed from the record and not included in the derivation of the annual ET values. For these periods, values were estimated based upon the number of missing values. Linear interpolation between values on either end of the period of removed records was used for short gaps of up to four hours in length. For gaps greater than four hours and up to 10 days, the record was estimated using averages of the same half hours for the day before and after the gap. Gaps were typically of short duration but on rare occasions, due to sensor malfunction, data gaps longer than 10 days would occur. These types of gaps were filled using the Reichstein method (Reichstein pers. comm., 2008). The Reichstein method is an automated algorithm (which can be found at http://www.bgc-jena.mpg.de/bgc-mdi/html/eddyproc/) that replaces the missing value by the average value under similar meteorological conditions within a

Table 3-2
ET-Measurement Site Instrumentation for EC Station, Meteorological Station, and Monitor Well

Measured Parameter	Instrument Type	Sensor Placement
EC Station		
Wind speed and air temperature	Campbell Scientific, Inc. CSAT3 3-D sonic anemometer	1 m (3.28 ft) above canopy cover for all sites except SV2b, which was placed 1.55 m (5.09 ft) above canopy[a]
CO_2 and H_2O vapor mass density and air pressure	LiCor, Inc. LI-7500 open-path IRGA	1 m (3.28 ft) above canopy cover for all sites except SV2b, which was placed 1.55 m (5.09 ft) above canopy[a]
Relative humidity and air temperature	Vaisala HMP45C capacitive relative humidity sensor	~ 1.5 to 2 m (4.92 to 6.56 ft) ags
Net radiation	Kipp & Zonen NR-Lite net radiometer	~ 1.5 to 2.5 m (4.92 to 8.20 ft) ags
Photosynthetically active radiation (PAR)	LiCor 190SA quantum sensor (400 to 700 nm)	1.0 to 2.5 m (3.28 to 8.20 ft) ags
Soil Moisture	Campbell Scientific, Inc. CS616 water-content reflectometer	2.5 cm (0.98 in.) bgs
Soil Temperature	Campbell Scientific, Inc. TCAV-Averaging soil thermocouple probe	2.5 to 5.0 cm (0.98 to 1.97 in.) bgs
Soil Heat Flux	Hukseflux HFP01SC-L thermopile gradient	8.0 cm (3.15 in.) bgs
Precipitation	Texas Electronics TE525 tipping bucket	1.37 to 2.50 m (4.50 to 8.17 ft) ags
Data collection and storage	Campbell Scientific, Inc. CR5000 data logger	---
Meteorological Station		
Air Pressure	Setra 278 barometric pressure sensor (600-1,100 millibars); Druck CS115	~ 0.5 to 1.0 m (1.64 to 3.28 ft) ags
Wind speed and direction	R.M. Young Wind Monitor (05103) propeller anemometer and wind vane	~ 2 m (6.56 ft) above canopy
Relative humidity and air temperature	Vaisala HMP45C capacitive relative humidity sensor	~ 1.5 to 2 m (4.92 to 6.56 ft) ags
Sun plus sky radiation	LI-COR, Inc. LI-200SZ pyranometer sensor (400 to 1,100 nm)	1 to 2 m (3.28 to 6.56 ft) ags
Soil Moisture	Acclima Digital TDT® Moisture sensor Time-Domain Transmissivity (TDT)	10 to 105 cm (3.94 to 41.34 in.) bgs
Precipitation	NOVALYNX 260-2510 8-in. diameter standard rain and snow gage Texas Electronics TE525 tipping bucket	80 to 100 cm (31.50 to 39.37 in.) ags 1.37 to 2.50 m (4.50 to 8.17 ft) ags
Data collection and storage	Campbell Scientific, Inc. CR10X data logger	---
Monitor Well		
Groundwater Level	Design Analysis DH-21 submersible pressure transducer and data logger	~<1.5 to 9.5 m (<5 to 31) ft bgs

[a]Placed at 1.55 m (5.09 ft) above canopy to minimize impact from a high enclosure of barb wire fencing around the site used to deter cattle.

Desert Research Institute and Southern Nevada Water Authority
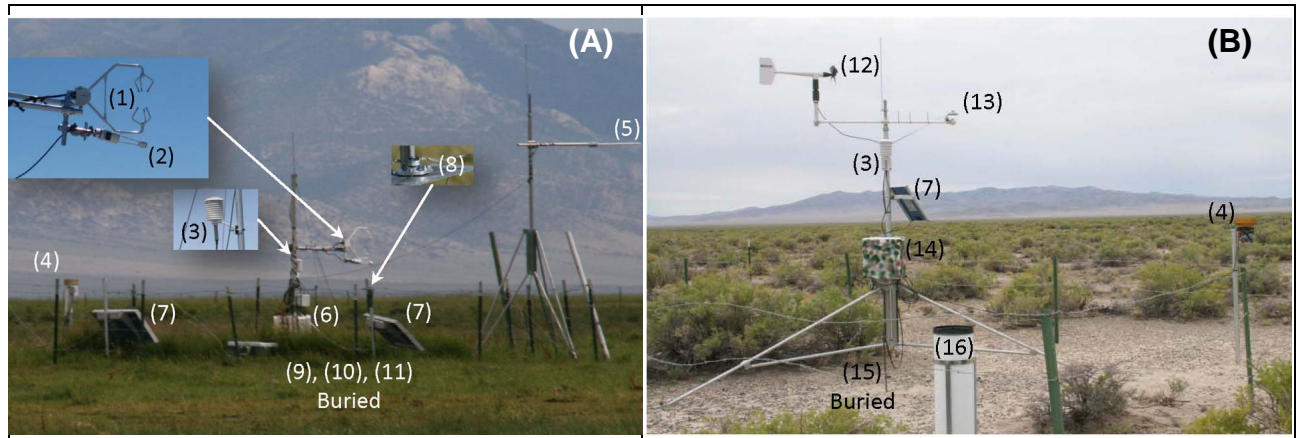
Note: (1) CSI CSAT3 3-D sonic anemometer; (2) LiCor 7500 open-path IRGA; (3) Vaisala HMP probe; (4) tipping bucket rain gage; (5) Kipp & Zonen NR-Lite net radiometer; (6) CSI CR5000 data logger; (7) solar panel; (8) LiCor 190SA quantum sensor; (9) CSI CS 616 water-content reflectometer; (10) CSI TCAV-Averaging soil thermocouple probe; (11) Hukseflux HFP01SC-L soil heat flux plates. (12) RM Young wind monitor; (13) LiCor 200SZ pyranometer sensor; (14) CSI CR10X data logger; (15) Acclima Digital TDT sensors; (16) bulk storage rain and snow gage.

Figure 3-2
Typical Deployment of EC (A) and Meteorological (B) Stations

designated time window. The time window is based on the availability of the similar meteorological data used to fill the gap, such as temperature or relative humidity (Reichstein et al., 2005, 2008). These methods are commonly applied in ET studies and are consistent with Fluxnet-Canada (2003) and Ameriflux guidelines (Munger and Loescher, 2006) as standard estimating techniques as described in Falge et al. (2001) and Reichstein et al. (2005). Sensor calibration was performed during the non-growing season when ET is minor or negligible (i.e., winter months), and the records for these missing periods were not estimated.

The performance of the EC stations was evaluated using data collected by sensors installed to independently measure the remaining parameters of the energy budget (H, R_n, G). These data were used to evaluate the overall effectiveness of the EC station to measure the full outgoing and incoming energy fluxes of the soil-plant-atmosphere boundary. The performance was assessed by rearranging the energy budget equation (Equation 3-1) in a form to compute the energy balance ratio (*EBR*) expressed by:

$$EBR = (H + L_eE)/(R_n - G) \qquad \text{(Eq. 3-3)}$$

An *EBR* of 1.00 implies that all of the available energy was accounted for in the energy budget measurements. Values larger or smaller than the optimum value of 1.00 imply that not all of the available energy was accounted for in one or more of the measured parameters. However, the *EBR* can be misleading because it is possible that the measurement error of one or more of the parameters can either: (1) offset the measurement error of the others, yielding an apparent *EBR* of 1.00; or (2) cause the *EBR* to diverge from 1.00. These errors can not be reconciled and attributed to a specific parameter; therefore, the *EBR* can only be used to provide a general sense of the EC station performance and the energy balance closure. Forcing energy balance closure by attributing the error to a particular parameter could lead to an overestimation/underestimation of that parameter. Instead, higher energy balance closure can be obtained, as this study has strived to do, by using up-to-date

Real-Time Processing
- Crosswind Correction (Liu et al., 2001)
- Automatic Time Delay Adjustment
- Gas Density Correction (Webb et al., 1980)

Raw flux and time series binary data collected from field

30-min flux data from data logger

Raw data conversion using Loggernet

10-Hz time series data

EdiRe Processing

Data Reduction

- Despiking (Højstrup, 1993)

Data Conversions and Corrections

- Coordinate Rotation (Wilczak et al., 2001)
- Gas Density (Webb et al., 1980)
- Bouyancy Flux (Schotanus et al., 1983)
- Frequency Response (Massman, 2000, 2001)
- Iteration of Interdependant Variables

QA/QC
- Vertical and Horizontal Integral Turbulence Tests (Foken and Wichura, 1996)
- N16200 and N17999 Tests (Vickers and Mahrt, 1997)
- Automatic Gain Control Flag
- Despiker Test (Vickers and Marht, 1997)
- Skewness Test (Vickers and Mahrt, 1997)
- Kurtosis Test (Vickers and Mahrt, 1997)
- Steady State Test (Foken and Wichura, 1996)
- CR5000 11.0 and 10.5 Battery Voltage Tests

Pass

Graphical Visual Inspection Process for Identifying Outliers

Fail

Gap Filling
- Linear interpolation method (using 1.5 hours before and after gap)
- Unbiased gap-filling method (using average between the same half hour for the day before and after the gap)
- Reichstein method (Reichstein et al., 2005)
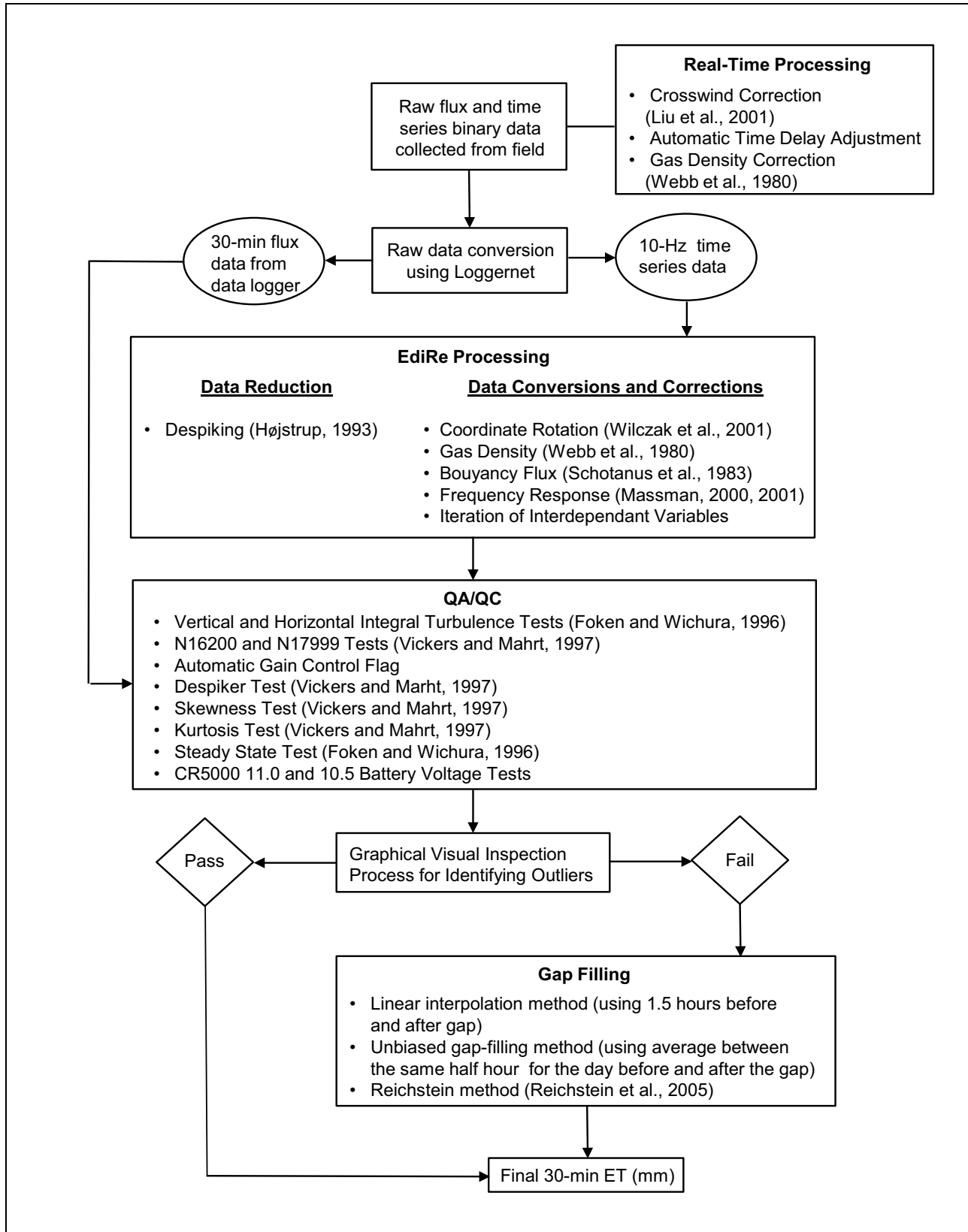
Final 30-min ET (mm)

Figure 3-3
Data Processing and Reduction Flowchart

sensor technology, instituting calibration and maintenance protocols, and implementing recent advancements in EC correction methods as recommended by Webb et al. (1980), Massman and Lee (2002), and Lee et al. (2004), and applying more stringent tests for data quality as recommended by Foken et al. (2004). Closing the energy balance is a common problem in energy budget methods, which is discussed in several papers (Wilson et al., 2002; Foken et al., 2006; Kohsiek, et al., 2007; Mauder et al., 2007; Oncley et al., 2007; Foken, 2008; and Wohlfahrt et al., 2009).

The *EBR* for the ET-measurement sites were computed using the half-hourly flux data. The average annual values for each station and corresponding years are listed in Table 3-3, with values ranging from 0.93 (SV1) to 1.58 (SV4), and an average value of 1.06 computed for all of the sites. At some sites the *EBR* exceeded 1.00 and, according to Hong (2008), this could be explained, in part, by an energy detection difference between the net radiation and sensible heat. That is, the high frequency measurement data may not reconcile the delayed effect that an abrupt drop in net radiation might have on the sensible heat flux (i.e., apparent *EBR* is larger). These *EBR* values are consistent with values reported by Moreo et al. (2007, p. 19) for the BARCASS sites, and better than those of Wilson et al. (2002) for 22 sites in a network of EC stations measuring long-term carbon and energy fluxes in contrasting ecosystems and climates. Moreo et al. (2007) reported an average *EBR* of 0.925 with a range of 0.82 to 1.06 for BARCASS sites, and Wilson et al. (2002, p. 228) reported a mean *EBR* value of 0.84 and a range of 0.34 to 1.69.

Table 3-3
Energy Balance Ratios

Site Name	2006	2007	2008	2009	2010	Average
WRV2	0.98[a]	0.91	0.89	1.02	0.97	**0.95**
SV1	0.89[a]	0.85	0.94	0.92	1.07	**0.93**
SV2b	---	0.94	1.13	1.08	1.25	**1.10**
SV3	---	0.97	0.99	0.99	1.04	**1.00**
SV4	---	1.37	1.68	1.69	---	**1.58**
SV5	---	1.03	1.05	1.10	---	**1.06**
SV6	---	1.01	1.02	1.12	---	**1.05**
SV7	---	0.93	0.94	1.09	---	**0.99**
SNV1	---	1.07	0.94	0.93	0.93	**0.97**
SNV2	---	0.94	0.96	0.90	0.96	**0.94**

[a]Devitt et al. (2008, p. 58).

3.1.4   Measurement Results

Time-series charts of total daily ET and reference ET are presented in Appendix A with mean daily depth-to-water values for each site and year for the period of record the stations were deployed. More detailed information on the data collection and processing is reported in Shanahan et al. (2011). Total annual ET rates in millimeters per year are listed for each station in Table 3-4. Table A-1 of Appendix A lists these values in feet per year.

Table 3-4
Annual ET (mm)

Site Name	2006	2007	2008	2009	2010	Period of Record[d]
WRV2	423.67[a]	219.46[b]	225.55	262.13	329.18	January 2006 - November 2010
SV1	240.79[a]	185.93[b]	192.02	234.70	292.61	January 2006 - November 2010
SV2b	---	1,088.14[b]	1,106.42	1,072.90	1,103.38	March 2007 - November 2010
SV3	---	240.79[b]	237.74	301.75	353.57	March 2007 - November 2010
SV4	---	749.81[c]	1,045.46[c]	1,277.11[c]	---	April 2007 - November 2009
SV5	---	243.84[c]	332.23[c]	490.73[c]	---	April 2007 - December 2009
SV6	---	207.26[c]	265.18[c]	390.14[c]	---	April 2007 - November 2009
SV7	---	131.06[c]	185.93[c]	243.84[c]	---	April 2007 - October 2009
SnV1	---	487.68[b]	316.99	259.08	310.90	May 2007 - November 2010
SnV2	---	198.12[b]	198.12	222.50	225.55	May 2007 - November 2010

Note: All annuals are January through December.
[a]Devitt et al. (2008, p. 40).
[b]These include additional data not reported in Devitt et al. (2008).
[c]Data collected by DRI personnel and processed by SNWA.
[d]Sites were not operational during periods of sensor calibration (typically late December through middle February).

The measured ET rates are consistent with measurements and estimates reported by previous investigators. Annual measurements for sites WRV2 and SV1 were compared to annual measurements from USGS BARCASS sites WRV-2 and SPV-1 (Moreo et al., 2007). Sites SV2b and SV4 were compared to use rates for comparable land-cover classes reported by Huntington and Allen (2010). The comparison is listed in Table 3-5 and presented in Figure 3-4.

As part of the USGS portion of the BARCASS, Moreo et al. (2007, p. 20) measured ET within the same areas (i.e., Spring and White River Valleys), for similar periods of data collection and land cover classes. BARCASS site WRV-2 was located near WRV2 within a similar medium-density stand of sagebrush and greasewood. BARCASS site SPV-1 was located near SV1 within a similar low-density stand of mixed phreatophytic vegetation. For the BARCASS sites, Moreo et al. (2007, p. 20) reported measured rates of 1.02 ft/yr and 0.84 ft/yr for WRV-2 and SPV-1, respectively, for the period September 1, 2005 through August 31, 2006. Annual ET measured at WRV2 and SV1 for 2006 was 423.67 mm/yr and 240.79 mm/yr, or 1.39 ft/yr and 0.79 ft/yr, respectively. Although the period of records and land cover classes were not exactly the same, the measured ET rates are comparable between the two studies.

The measured ET rates for wetland/meadow sites, SV2b and SV4, compare favorably to estimates of ET reported by Huntington and Allen (2010, Appendix 14, p. 238-248) for Spring Valley. The SV2b and SV4 sites are located in meadowlands with groundwater at or near the ground surface (Figures A-3 and A-5). For much of the growing season, the SV2b site typically has standing groundwater over part of the footprint area. The SV2b site correlates to the "highly-managed pasture grass" and SV4 site to the "low-managed pasture grass" categories of Huntington and Allen (2010). For these categories, Huntington and Allen (2010) estimated annual rates of 3.6 ft/yr and 3.0 ft/yr,

Table 3-5
Comparison of Annual ET Rates

Source	Site Name	Land Cover Description	Period of Record	ET (mm)	ET (ft)
This Study	WRV2	55% cover; predominantly sagebrush and greasewood with minor amounts of shadscale	January 2006 - December 2006	423.67	1.39
Moreo et al. (2007)	WRV-2	Moderately dense desert shrubland	September 1, 2005 - August 31, 2006	309.37	1.02
This Study	SV1	27% cover; predominantly sagebrush with rabbitbrush and greasewood; shadscale and buckwheat also present	January 2006 - December 2006	240.79	0.79
Moreo et al. (2007)	SPV-1	Sparse desert shrubland	September 1, 2005 - August 31, 2006	254.51	0.84
This Study	SV2b	Irrigated pasture/grassland; 100% cover of perennial grasses	March 2007 - November 2010	1,094	3.59
Huntington and Allen (2010)	---	Highly-managed pasture grass	---	1,097	3.6
This Study	SV4	Irrigated pasture/grassland; 100% cover of perennial grasses	April 2007 - November 2009	1,024	3.36
Huntington and Allen (2010)	---	Low-managed pasture grass	---	914	3.0
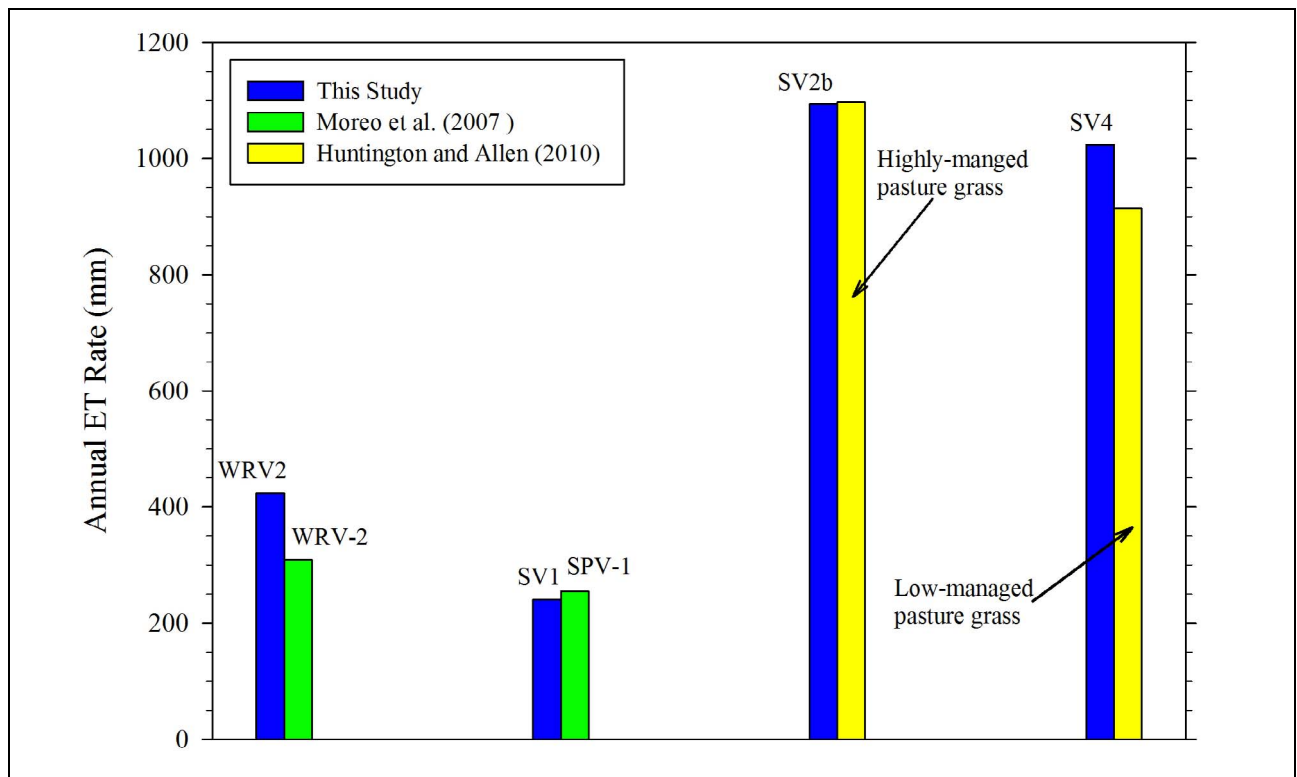
Figure 3-4
Comparison of Annual ET Rate

respectively. The average annual ET measured at SV2b and SV4 for the five-year period of record was 1,094 mm/yr and 1,024 mm/yr, or 3.59 ft/yr and 3.36 ft/yr, respectively.

4.0   SATELLITE IMAGERY ACQUISITION AND PROCESSING

4.1   Satellite Imagery Acquisition

Landsat TM 5 scenes were acquired from the USGS Earth Resources Observation and Science (EROS) Data Center in Sioux Falls, South Dakota. These data are currently provided at no cost with a 30 m by 30 m spatial pixel resolution. Only scenes with less than 30 percent cloud cover were acquired for the growing season (late April through the middle of September) for each year; see Table 4-1 below for a list of specific dates. The Landsat TM 5 satellite acquires scenes by paths and rows. Repeat coverage for each path occurs every 16 days. Scenes were acquired for rows 32 and 33 on path 39 to encompass both Spring and Snake Valleys, and row 33 on path 40 for White River Valley. Data acquisition of Landsat TM paths 39 and 40 are offset by seven days.

Table 4-1
List of Landsat TM 5 Scene Dates for Each Year
by Landsat TM 5 Path/Row

Year/Path-Row	Path 39, Rows 32, 33 (Spring and Snake Valleys)	Path 40, Row 33 (White River Valley)
2006	5/12, 6/29, 7/15, 8/16, 9/1, 9/17	5/19, 6/4, 6/20, 8/7, 9/8, 9/24
2007	4/29, 5/15, 5/31, 6/16, 7/2, 7/18, 8/19, 9/20	5/6, 5/22, 6/23, 7/9, 8/10, 9/27
2008	5/1, 5/17, 6/18, 8/21, 9/6, 9/22	5/8, 6/9, 6/25, 7/11, 8/12, 8/28, 9/13
2009	4/18, 6/21, 7/7, 7/23, 9/9, 9/25	5/11, 6/28, 7/14, 8/15, 9/16
2010	5/7, 6/8, 8/11, 8/27, 9/12	5/14, 7/1, 7/17, 8/2, 9/3

4.2   Satellite Imagery Processing

The Landsat TM 5 image analysis followed four basic steps: (1) radiometric calibration, atmospheric correction and normalization of each Landsat scene (60 scenes total); (2) calculation of an NDVI image for each Landsat scene date; (3) identification, masking and back-filling of any clouds and cloud shadows present in each scene; and (4) calculation of an average growing season NDVI image (AvgNDVI) for each year. The details of the image analysis are provided in the following sections for each of the four basic steps. The image analysis was performed using ENVI software (ENvironment for Visualizing Images, ITT™ Visual Information Solutions, Boulder, Colorado) in a consistent manner with standardized methods to ensure data comparability. Linear regression analyses required for the empirical line method atmospheric correction and normalization were performed using SigmaStat statistical software (Systat Software Inc., Chicago, Illinois).

4.2.1   Calibration, Atmospheric Correction, and Normalization

The first step in processing the images was a calibration to top-of-atmosphere (or at-sensor) radiance performed by the ENVI Landsat TM 5 calibration subroutine. Top-of-atmosphere radiance is the spectral radiance measured at the Landsat sensor's aperture in units of $W\ m^{-2}\ sr^{-1}\ \mu m^{-1}$, which is the radiance of the land surface plus any atmospheric affects between the land surface and the satellite. The ENVI calibration subroutine used the equations, gains and offsets defined by Chander et al. (2009) for the radiometric calibration of Landsat TM data. This subroutine therefore converted the digital numbers provided by EROS for each image pixel to radiance values. The second step was atmospheric correction, image normalization and conversion to ground reflectance values. The empirical line method was selected for this project (Farrand et al., 1994 and Smith and Milton, 1999) because of the availability of reasonably unchanging ground areas with dark to light spectral reflectances. This approach was based on the regression of dark and light ground target spectra to image radiance values for the same areas. For each image date, the coordinates for the ground target locations were used to collect the image radiance values for the 2-4 corresponding pixels (Table 4-2). Field spectra acquired with a FieldSpec Pro (Analytical Spectral Devices, Inc., Boulder, Colorado) (with 1 nm spectral resolution) were converted to Landsat TM bandwidths with the ENVI Spectral Library Resampling tool, which employs a Gaussian model based on the TM band wavelength and full-width at half maximum (FWHM) sensitivity of the Landsat TM detector for the conversion. The resulting converted field reflectance spectra and corresponding average Landsat TM pixel radiances were used to develop regression equations. The regression equations were entered one band at a time into the ENVI Band Math subroutine to atmospherically correct all pixels within the images to ground reflectance values. To ensure that differences in sun angle throughout the year did not impact further image analysis, all images were corrected with regression equations based on the field spectra from June 20, 2006, which provided simultaneous normalization of all images.

Table 4-2
The Upper Left (NW) and Lower Right (SE) Coordinates
for the Ground Calibration Targets

	Upper Left[a]		Lower Right[a]	
Site Name	Northing	Easting	Northing	Easting
Igneous Rock	4,241,412	667,138	4,241,362	667,162
Gravel Pit	4,244,038	670,262	4,243,988	670,312
Bright Soil 1	4,247,388	665,212	4,247,338	665,238
Bright Soil 2	4,254,112	669,062	4,254,062	669,088

[a]All coordinates are UTM NAD83, Zone 11.

4.2.2   Generation of NDVI Images

The NDVI has previously been demonstrated to be a reasonable predictor of green vegetation cover and correlated with ET in other arid regions (e.g., Tucker, 1979; Groeneveld et al., 2007). As mentioned in Section 2.2.2 the NDVI provided more accurate predicted ET values than the EVI using Landsat TM data for this study area. In addition, the NDVI has been widely used and is the most

frequently published VI. Therefore the NDVI for empirical prediction of ET was selected for this study and the NDVI was calculated based on Rouse et al. (1974) as follows:

$$NDVI = (R_{NIR} - R_{RED})/(R_{NIR} + R_{RED}) \qquad \text{(Eq. 4-1)}$$

where,

R = Reflectance for the waveband indicated by each subscript
NIR = Near infrared waveband from 0.76 to 0.90 nm
RED = Red waveband from 0.63 to 0.69 nm.

The ENVI Band Math subroutine was used to calculate an NDVI image for each Landsat TM 5 image date.

4.2.3   Identification of Clouds and Cloud Shadows

Clouds and cloud shadows were identified for each image date by a series of band thresholds using the ENVI Region-of-Interest (ROI) tool set. The image dates that were identified for cloud and cloud shadow replacement are listed in Table 4-3 for each valley. The cloud and shadow areas were identified to allow replacement of these pixels within a particular image with average pixel values from all or a subset of cloud-free image dates. Clouds were best identified by setting a reflectance threshold of greater than approximately 0.35 for all pixels in the atmospherically corrected blue band (Landsat TM band 1). The specific threshold value for each image was determined via an iterative process where a color composite image (bands 4, 3 and 1 as red, green and blue) was carefully examined to ensure that the maximum amount of cloud pixels were identified with either none or a very minimal amount of bright soil pixels included with the cloud pixels. In some instances, another ROI was hand digitized and intersected with the cloud threshold ROI to ensure that bright soil areas were not included in the resulting cloud ROI. Cloud shadows, particularly cumulus cloud shadows, were easily identified by thresholding all negative or very low NDVI image pixels. In a few instances, hand digitized ROIs had to be created and intersected with the shadow ROI to ensure that dark surface features were not included as cloud shadow. When cirrus clouds were present in the image, it was difficult to define discrete thresholds for identifying areas covered by thin clouds; therefore, hand digitizing of cloud and cloud shadow boundaries was required. Figure 4-1 provides a step-by-step visual representation of the process.

Table 4-3
List of Images Requiring Cloud Removal and Replacement for Each Valley by Year

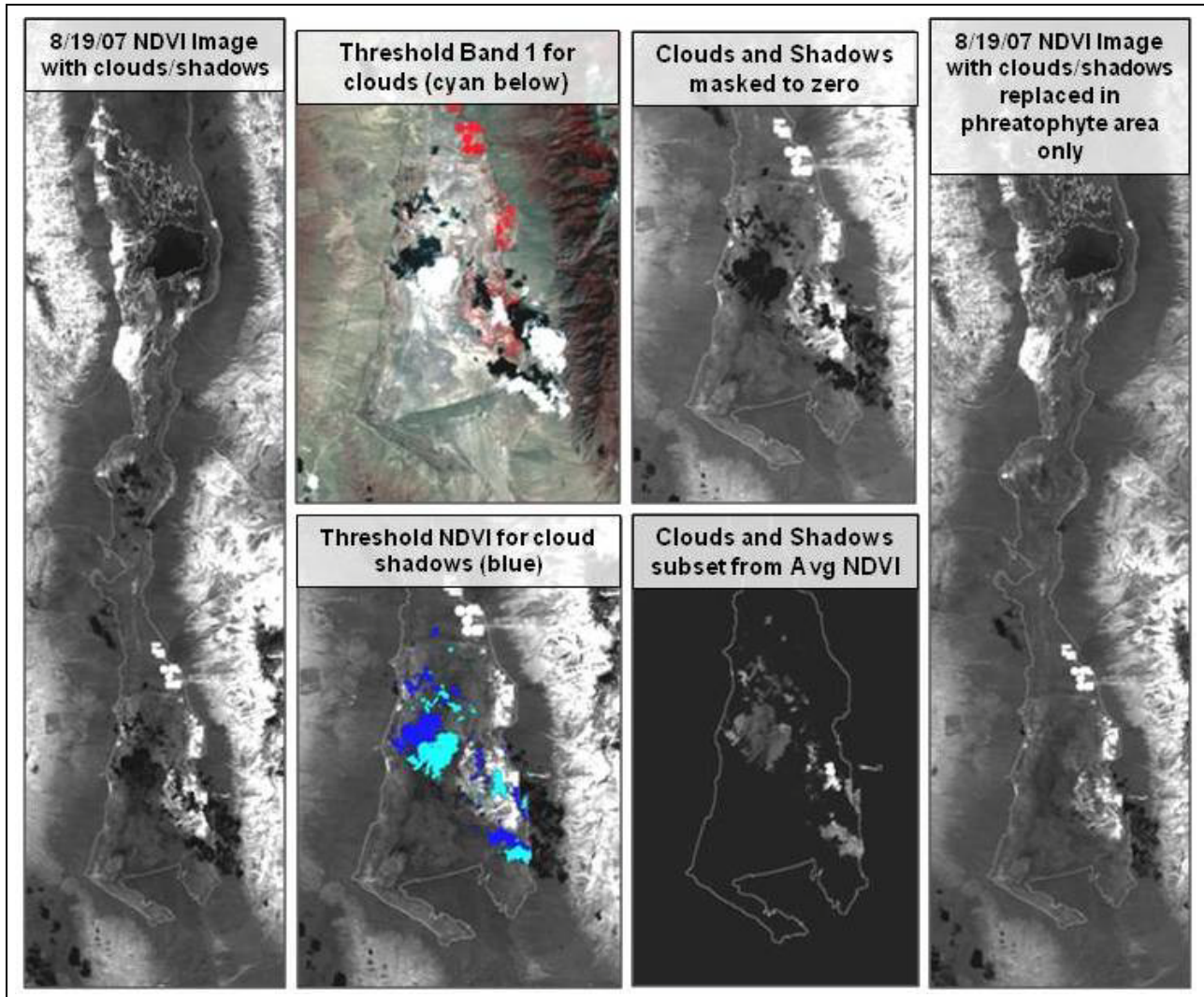| HA Name	2006	2007	2008	2009	2010
Snake Valley	---	8/19	5/1, 9/22	4/18, 6/21, 7/23	8/27
Spring Valley	6/29	8/19, 9/20	5/1, 9/22	7/23	6/8, 8/27
White River Valley	5/19, 8/7	6/23	7/11	6/28, 8/15	5/14, 7/17, 8/2

Figure 4-1
Subsets for Spring Valley Demonstrate the Cloud and
Cloud Shadow Identification and Pixel Replacement Process

4.2.4   Calculating Growing-Season Average NDVI Image

To calculate an average NDVI image, each pixel within the valleys had to represent the actual surface characteristics and e.g., not cloud covered or cloud shadowed. For image dates where clouds were present, the corresponding pixels had to be replaced with an appropriate value that would result in an as accurate as possible average image. A subset of cloud-free images from across the growing period of each year were used to calculate a preliminary average NDVI image. The ROI's that had been previously defined for cloud covered areas were then used, via the ENVI masking subroutine, to create images that contained only the preliminary average pixel values for the cloud or shadow ROI's. The same ROI's were also used to mask and convert all pixels within the cloud image where clouds or shadows were present to a zero value. The resulting images were then added together. All merged images as well as complete, cloud-free images from the growing period of each year were then averaged using the ENVI layer stacking and band math subroutines. The layer stacking subroutine

allows the user to transform georeferenced images that may have different pixel resolutions, extents or projections into one multiband image file with a common pixel size, extents and coordinate projections. After layer stacking, the band math subroutine was used to add all image bands together and then divide by the number of bands to create a growing-season average NDVI image.

4.3   ET-Station Footprint Analysis

In Arnone et al. (2008), the footprint for each site was calculated using the footprint model of Hsieh et al. (2000) to estimate the upwind distance and compass direction that represented 90 percent of the surface flux for each half-hour period ($X_{90\%}$) (Equation 4-2):

$$X_{90\%} = \frac{-\mathrm{D}|L|^{(1-P)}Z_u^P}{k^2 \ln(0.90)}$$
(Eq. 4-2)

where k is the von Karman constant (0.4), L is the Obukhov length, and Z_u is the length scale calculated as:

$$Z_u = \frac{Z_m u k}{u_*}$$
(Eq. 4-3)

where Z_m is the measurement height, u is the mean wind speed, and D and P are stability-dependent coefficients, for example,

$D = 0.28$; $P = 0.59$ for unstable conditions
$D = 0.97$; $P = 1.00$ for near-neutral conditions
$D = 2.44$; $P = 1.33$ for stable conditions

Atmospheric stability is dependent upon the temperature of rising air in comparison to the temperature of the surrounding air that the rising air passes through. If the surrounding air temperature does not change rapidly as the rising air passes through it then the atmosphere is said to be stable. If, however, the surrounding air temperature changes rapidly in response to the rising air temperature then the condition is unstable. A neutral or near neutral condition occurs when the average rate of temperature decrease of a parcel of rising air (lapse rate) is the same as the rate of temperature decrease of a rising dry parcel of air (dry-adiabatic lapse rate). The stability-dependent coefficients used in the calculation are determined by the value of $|z_u/L|$ or the absolute value of the length scale (based on measurement height) divided by the Obukhov length (based on friction velocity, mean air temperature, gravitational constant, von Karmen's constant, and the average temperature fluctuation) or by the Obukhov length alone. Neutral or near neutral conditions are defined by $|z_u/L| < 0.04$, whereas a value of $L = -50$ m represents an unstable condition and $L = -100$ m represents a stable condition. The resulting upwind distance and azimuth were then plotted in ArcGIS as an x, y location from each tower's central global positioning system coordinate; e.g., distance and azimuth from the tower center were plotted and thereby yielding points with individual x, y coordinates (Figure 4-2). During a one-year period there are numerous distance/
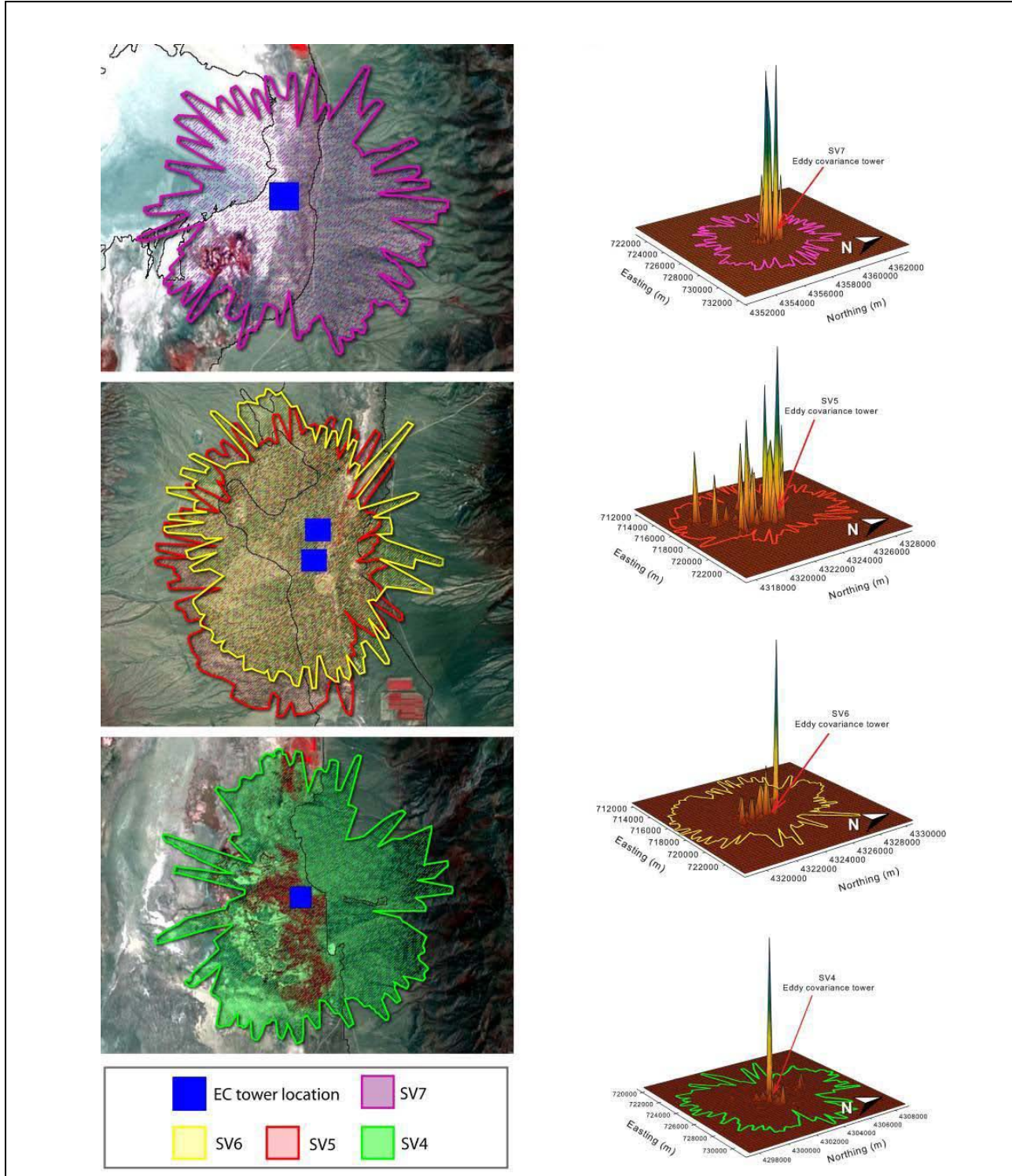
Source: Arnone et al. (2008).
Note: The location and size of the footprint for each of the four EC sites located in Spring Valley between April 20, 2007 and April 20, 2008 are depicted in the left panel. In the right panel, three-dimensional mesh images depict the level of representation of 250 x 250 m grid cells (cell size for graph preparation) within each EC tower footprint to annual ET over the study year. The footprint extent encompassed the area that contributed 90 percent of the ET fluxes during the year.

Figure 4-2
Footprint Extents for Selected EC Stations in Spring Valley (April 2007-April 2008)

azimuth (e.g., geographic coordinates) points that fall within a single 30 × 30 m grid cell, e.g., corresponds to a Landsat 5 TM pixel size.

In the original footprint calculation (Arnone et al., 2008), growing season average NDVI was calculated by averaging all pixels within the footprint boundary. The pixels within the footprint boundary were not weighted for their contribution to ET (i.e., pixels that contributed more ET throughout the year carried an equal weight to pixels that contributed little when calculating the average footprint NDVI). Given that some areas within the footprint clearly contribute more to measured ET than other areas within the footprint, a weighted average NDVI would better represent the vegetation components imparting the largest ET signal measured by the EC station.

To create an appropriate weighting factor for each NDVI image pixel, the number of points that fell within a single 30 m grid cell received a value of one for each point. Point assignment occurred during the ArcGIS point to raster conversion where the number of points within a grid cell were summed so that the value assigned was equal to the number of points that fell within that particular cell. Thus, if 12 points fell within a single 30 × 30 m cell, that cell received a value of 12. If no points fell within a particular grid cell (pixel) then a value of zero was assigned. The resulting footprint "image" therefore resembles a "shotgun" scatter of pixels around each station location (Figure 4-3). The "count" footprint image was used in a multiplication band math procedure with subsets for each station location from the average growing season NDVI image. The resulting weighted NDVI values were summed and divided by the total number of counts for each station to calculate the weighted average growing season NDVI within each EC-station footprint.
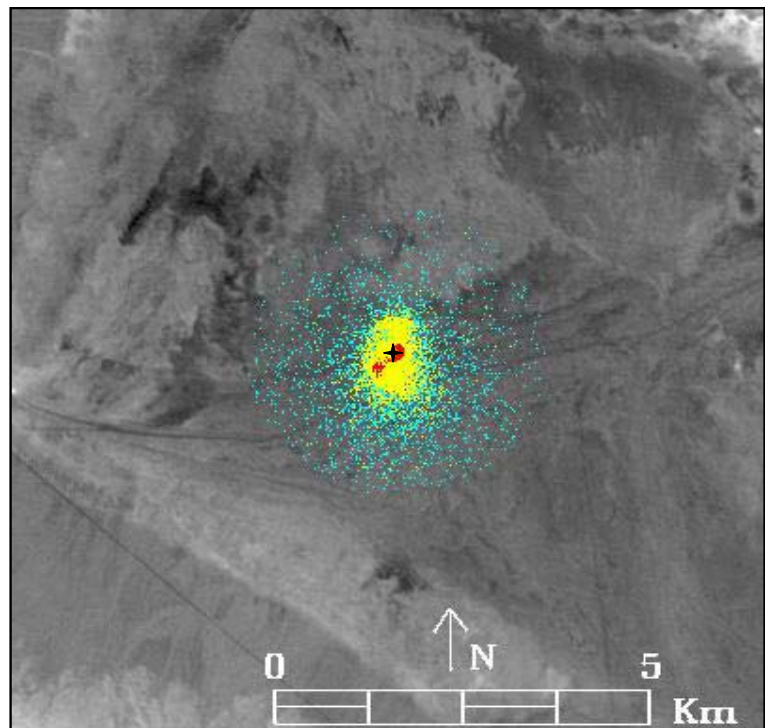
Note: The 2007 footprint for the Spring Valley 1 (SV1) EC station is depicted within the 2007 growing season average NDVI image. Each of the color points is assigned a count for the number of times that location contributed to ET measured by the EC station within the year. The cyan color represents 1-2 counts, yellow is 2-20 counts and red is greater than 20 counts. The location of the SV1 tower is marked with a black plus "+".

**Figure 4-3
Footprint for SV1 EC Station**

This Page Left Intentionally Blank

5.0 ANNUAL ET VERSUS NDVI REGRESSION ANALYSIS

Regression analysis was performed between annual ET (from EC-station measurements) and footprint-weighted growing season average NDVI values, using SigmaPlot 11 statistical software. The purpose of this analysis was to generate a regression equation that could be used to generate spatial distributions of annual ET from which estimates of total annual ET for the groundwater discharge areas of White River and Spring Valleys could be derived.

5.1 Data Evaluation

Footprint-weighted average NDVI values were extracted from each AvgNDVI image for each year and EC-station location. These data along with their respective annual ET values are listed in Table 5-1 and presented in Figures 5-1 and 5-2.

Table 5-1
Footprint-Weighted Average NDVI and Annual ET for ET-Measurement Sites
Located in Snake, Spring, and White River Valleys, Nevada

Site	Footprint-Weighted Average NDVI					Measured Annual ET (mm)				
	2006	2007	2008	2009	2010	2006	2007	2008	2009	2010
WRV2	0.0934	0.0808	0.0937	0.0924	0.0700	423.67	219.46	225.55	262.13	329.18
SV1	0.0483	0.0533	0.0616	0.0634	0.0658	240.79	185.93	192.02	234.70	292.61
SV2b	---	0.4029	0.3199	0.4720	0.4103	---	1,088.14	1,106.42	1,072.90	1,103.38
SV3	---	0.0586	0.0487	0.0549	0.0786	---	240.79	237.74	301.75	353.57
SV4	---	0.2823	0.2967	0.4363	---	---	749.81	1,045.46	1,277.11	---
SV5	---	0.0776	0.0859	0.1142	---	---	243.84	332.23	490.73	---
SV6	---	0.0778	0.0827	0.1087	---	---	207.26	265.18	390.14	---
SV7	---	0.0460	0.0395	0.0490	---	---	131.06	185.93	243.84	---
SnV1	---	0.1104	0.1143	0.1025	0.1027	---	487.68	316.99	259.08	310.90
SnV2	---	0.0715	0.0624	0.0561	0.0620	---	198.12	198.12	222.50	225.55

Figures 5-1 and 5-2 depict the time-series plots of both footprint-weighted average NDVI values and annual ET values, respectively, by year for all stations. The footprint-weighted average NDVI values are fairly consistent from year to year except for the SV2b station for 2008 and 2009, and the WRV2 station for 2010. As compared to the period-of-record average, SV2b has a significantly decreased value for 2008 (0.08, or 20 percent), and a significantly increased value for 2009 (0.071, or 18 percent). For WRV2, the NDVI average for 2010 did not include NDVI values for peak-ET months due to excessive cloud cover; therefore, this average is significantly lower that than the period of record average (0.016, or 19 percent).
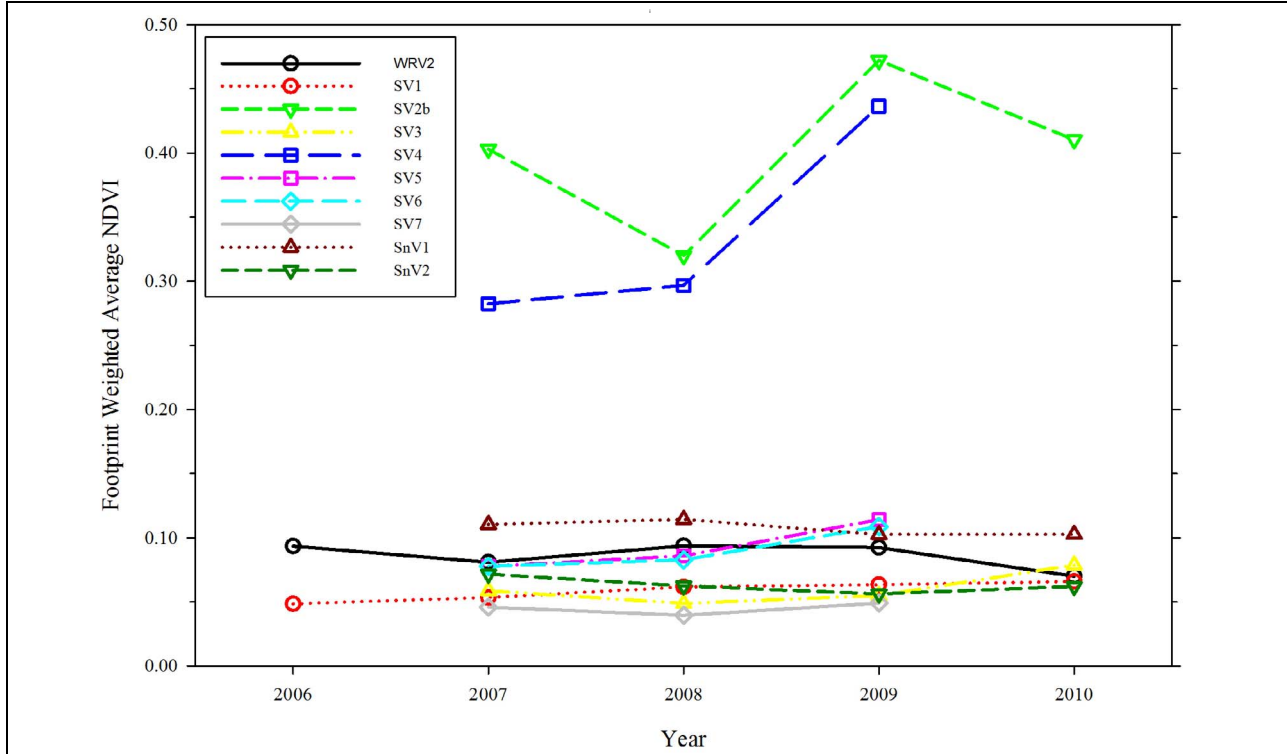
Figure 5-1
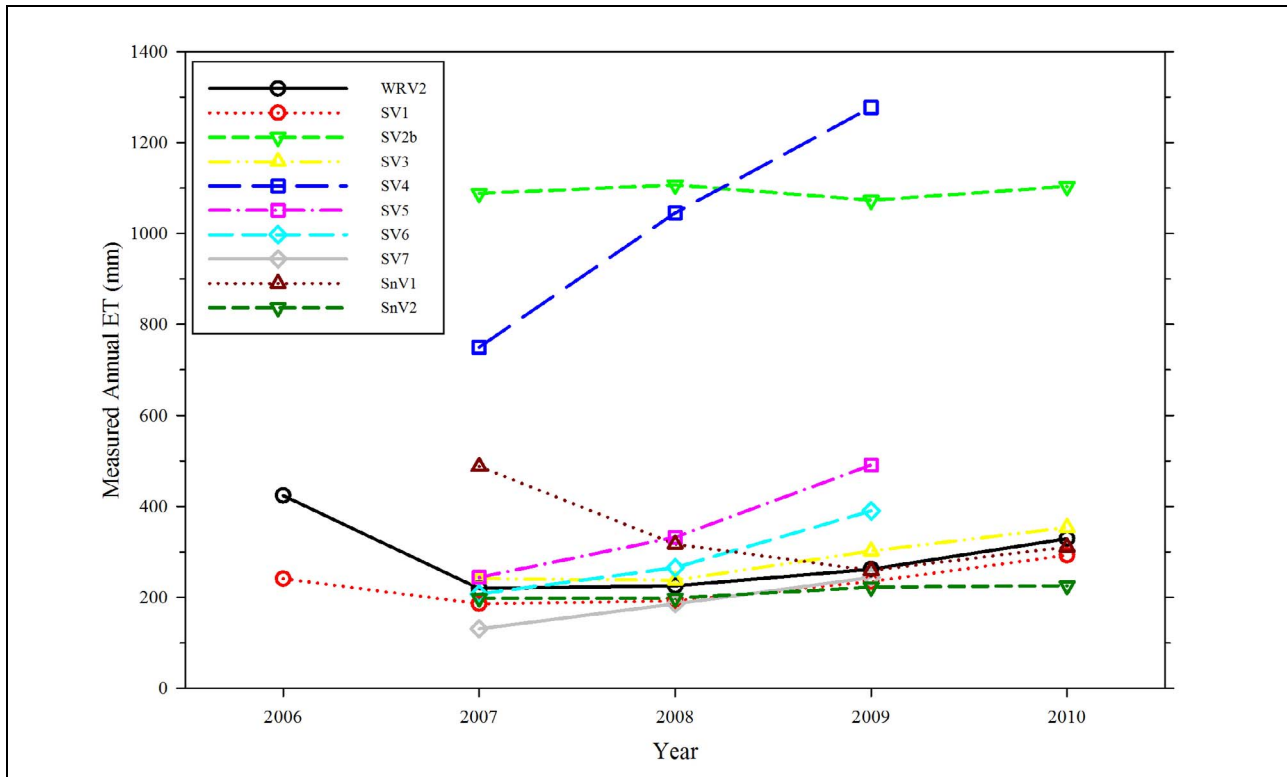**Time-Series Plots of Footprint-Weighted Average NDVI**

Figure 5-2
Time-Series Plots of Measured Annual ET

A scatter-plot depicting the footprint-weighted average NDVI and annual ET for all measurement sites and years was prepared to qualitatively assess the relationship between these two variables, and is presented in Figure 5-3. Based on this plot, the data follow a linear trend suggesting that a linear relationship exists between the two variables. Figure 5-3 also reveals a significant degree of scatter among the wetland/meadow data points, particularly the SV2b station which exhibits significant variability in the footprint-weighted average NDVI for similar values of annual ET (see also Figures 5-1 and 5-2). A strong relationship is apparent for all of the shrub data points which are clustered in the lower left corner of the graph.
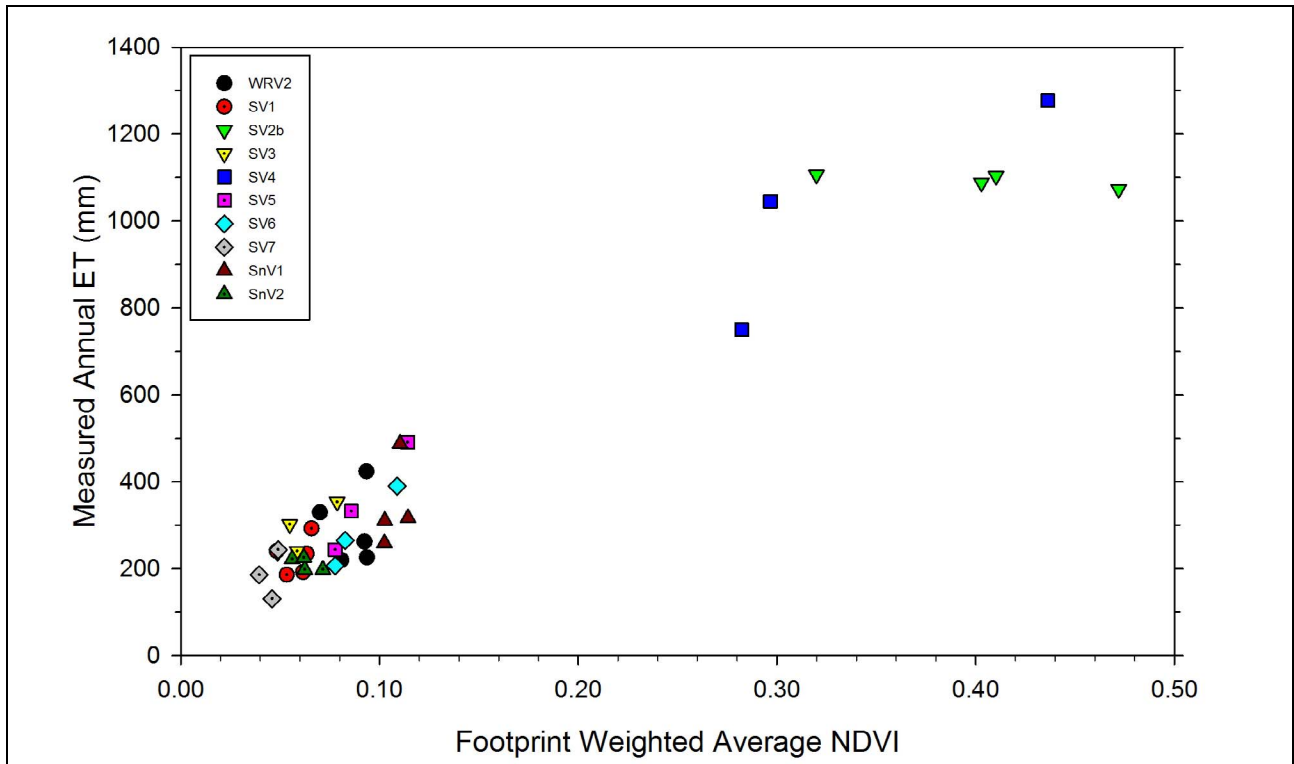

Figure 5-3
Scatter Plot of Annual ET and Footprint-Weighted Average NDVI

5.2   *Regression Analysis and Accuracy Assessment*

A linear-regression analysis was performed by setting the annual ET measurement as the dependent variable and the corresponding footprint-weighted average NDVI value as the independent variable. The regression statistics and the residuals between predicted and measured values were assessed to evaluate the regression-model fit. An accuracy assessment was performed by comparing predicted annual ET values to measured annual ET values for data points reserved from the regression analysis data set. The following sections describe the data selection, linear-regression analysis, and accuracy assessment.

5.2.1 Data Selection

Of the 38 data points available for the regression analysis, 31 were included. Seven data points were removed from the regression analysis and reserved for an independent accuracy assessment. The descriptive statistics for all data points were carefully examined to ensure that the reserved points encompassed the range in NDVI and annual ET values, as well as the mean and median, for all measurement sites and years. These data points also represented sites encompassing the full range of land-cover classifications (low, moderate and dense shrub and wetland/meadow). The absolute minimum and maximum values of the data set were not reserved for the accuracy assessment to ensure that the regression equation would encompass the entire data range for the five year period. No data points were reserved for accuracy assessment from 2006 because there were only two data points for that year. The data points removed from the regression analysis included: SnV1 and SV5 in 2007; WRV2 and SV7 in 2008; SV2b and SV6 in 2009; and SV3 in 2010.

5.2.2 Regression Analysis

Using SigmaPlot 11 software, a linear regression was performed using the 31 data points described in the previous section. Figure 5-4 presents the data with the best-fit line expressed by Equation 5-1 as follows:

$$\text{Annual ET (mm)} = 65.426 + (2,749.087 \times \text{Avg NDVI}); (n = 31, r^2 = 0.953) \qquad \text{(Eq. 5-1)}$$

The regression model (Equation 5-1) was evaluated by reviewing the residuals (measured minus predicted annual ET values) to identify any trends and whether or not the residuals are normally distributed. The residuals are listed in Table 5-2.

A plot of the residuals versus the predicted annual ET (Figure 5-5) indicates there is no discernible bias in the regression model because of the random nature of the residual distribution about the zero line. This indicates that the model does not have a bias towards over- or under-predicting ET rates. Figure 5-5 presents a second plot of the residuals versus land-cover classification, which indicates there may be a slight bias associated with the land-cover classifications because the residuals appear to increase from the bare-soil/low-vegetation class to the wetland/ meadow class. However, if the residual is evaluated as a percentage of the annual measured ET, the opposite trend is observed because the percentage decreases from the bare-soil/low- vegetation class to the wetland/meadow class.

A normal quantile plot was prepared to assess whether or not the residuals are normally distributed. Normally-distributed residuals, as shown in this case, indicate that the regression model provides an excellent representation of the relationship between measured annual ET and footprint-weighted average NDVI. Figure 5-5 presents a plot of the residuals versus the normal quantiles, along with the best-fit line. The data appear to follow a linear trend, and the R^2 of the best-fit line (0.94) confirms it. Theoretically, the closer the correlation coefficient (R) is to 1, the more likely the probability distribution is normal. In this case, R equals 0.97, which leads to the conclusion that the residuals are normally distributed.
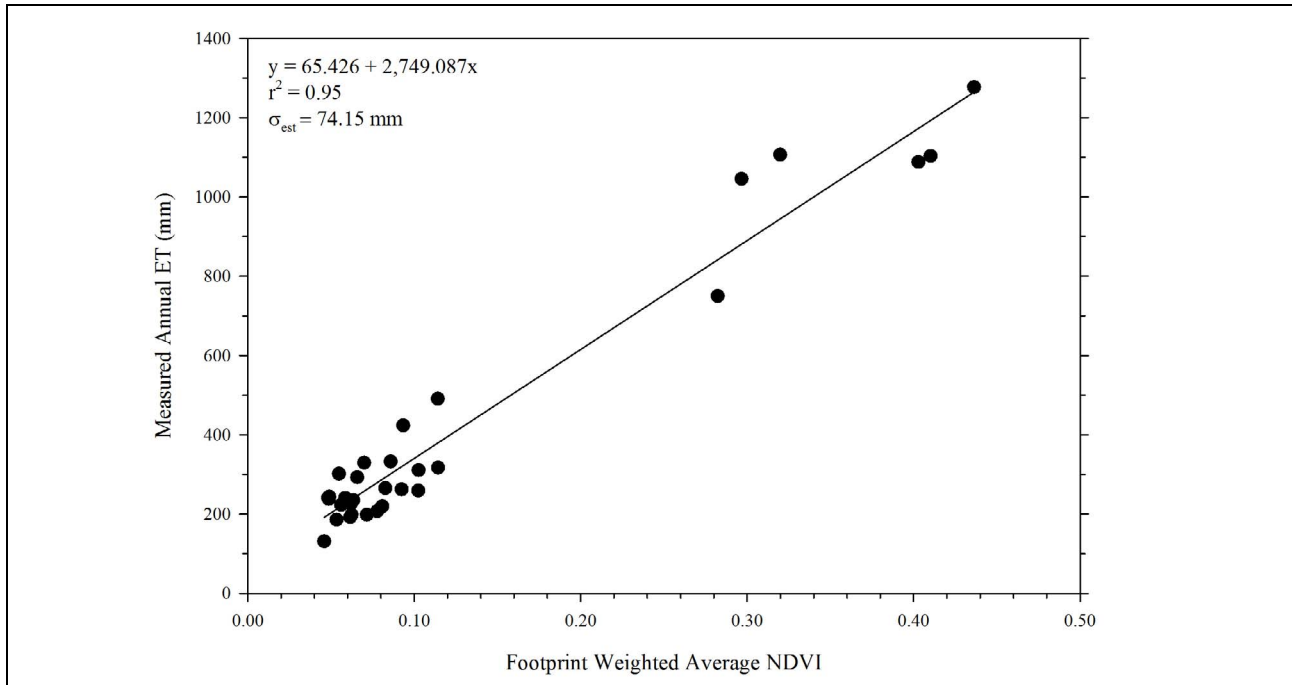
Figure 5-4
Footprint-Weighted Average NDVI Versus Annual ET Linear-Regression Relationship

The standard error of the estimate (σ_{est}) for the regression model was calculated as the square root of the sum of squared residuals divided by the number of data points (n=31) minus the degrees of freedom (df=1). The resultant value is a measure of the accuracy of the prediction, in this case the value is 74.15 mm.

Finally, a second linear-regression analysis was performed using all of the data points (the original 31 plus the 7 reserved for the accuracy assessment) to allow comparison of the two models (n=31 versus n=38) to verify that removal of the seven points did not have a significant effect on the regression relationship. Figure 5-5 presents this comparison which reveals that the two relationships are quite similar. The primary difference is a slightly increased slope and slightly decreased intercept for first regression (n=31), which is most likely due to the removal of one wetland/meadow data point for use in the accuracy assessment. This point (SV2b, 2009) has a significantly higher footprint-weighted average NDVI value than other data with a similar annual ET value. In the second regression model (n=38), this data point negatively affects the regression by reducing the R^2 to 0.94.

5.2.3   Accuracy Assessment

As stated in the previous sections, seven data points were excluded from the regression analysis so that an independent accuracy assessment of model predictions could be performed. For these remaining data points, the predictive error was computed as the difference between the annual predicted ET minus the annual measured ET. These values are listed in Table 5-3 with the percent error of the predictions. For Spring Valley, the percent error ranges from 7 percent to 26 percent, with an average value of about 15 percent. For Snake and White River valleys, the percent errors are 32 percent and 30 percent, respectively.

Table 5-2
Residual Difference of Annual Measured ET minus Annual Predicted ET

HA Name	Land Cover	Station Name	Year	Annual Measured ET (mm)	Annual Predicted ET (mm)	Residual[a] (mm)
White River Valley	Phreatophyte/Medium Density Vegetation	WRV2	2006	423.67	322.22	101.46
			2007	219.46	287.61	-68.15
			2009	262.13	319.53	-57.40
			2010	329.18	257.95	71.23
Spring Valley	Bare Soil/Low Density Vegetation	SV7	2007	131.06	191.75	-60.68
			2009	243.84	200.13	43.71
	Phreatophyte/Medium Density Vegetation	SV1	2006	240.79	198.33	42.46
			2007	185.93	212.04	-26.11
			2008	192.02	234.80	-42.78
			2009	234.70	239.66	-4.97
			2010	292.61	246.36	46.25
		SV3	2007	240.79	226.42	14.38
			2008	237.74	199.43	38.31
			2009	301.75	216.22	85.53
		SV5	2008	332.23	301.44	30.80
			2009	490.73	379.27	111.45
		SV6	2007	207.26	279.26	-72.00
			2008	265.18	292.75	-27.58
	Wetland/Meadow	SV2b	2007	1,088.14	1,173.13	-85.00
			2008	1,106.42	944.80	161.62
			2010	1,103.38	1,193.25	-89.88
		SV4	2007	749.81	841.49	-91.68
			2008	1,045.46	881.02	164.45
			2009	1,277.11	1,264.96	12.15
Snake Valley	Phreatophyte/Medium Density Vegetation	SnV1	2008	316.99	379.70	-62.71
			2009	259.08	347.21	-88.13
			2010	310.90	347.66	-36.77
	Bare Soil/Low Density Vegetation	SnV2	2007	198.12	262.01	-63.89
			2008	198.12	236.93	-38.81
			2009	222.50	219.55	2.96
			2010	225.55	235.78	-10.23

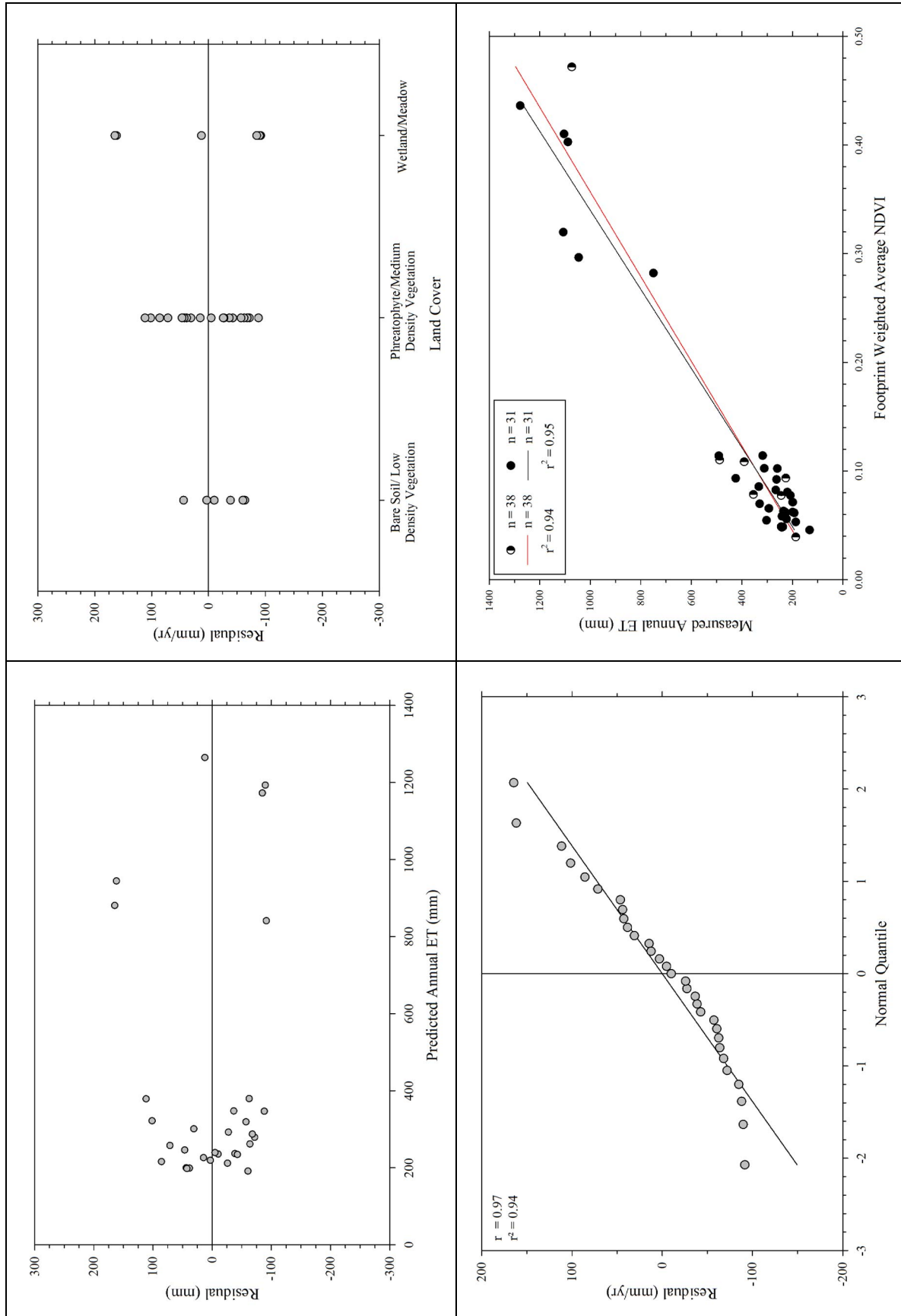[a]±0.01 mm due to rounding. Values represent a larger number of decimal places.

Figure 5-5

Regression Model Residual Plots and a Comparison of Sample Size (n=31 versus n=38)

Table 5-3
Difference of Annual Predicted ET minus Annual Measured ET

HA Name	Land Cover	Station Name	Year	Annual Predicted ET (mm)	Annual Measured ET (mm)	Predictive Error (mm)	Percent Error (%)
Snake Valley	Phreatophyte/Medium Density Vegetation	SnV1	2007	368.93	487.68	-118.75	32
Spring Valley	Bare Soil/Low Density Vegetation	SV7	2008	174.01	185.93	-11.92	7
	Phreatophyte/Medium Density Vegetation	SV3	2010	281.50	353.57	-72.07	26
		SV5	2007	278.76	243.84	34.92	13
		SV6	2009	364.25	390.14	-25.89	7
	Wetland/Meadow	SV2b	2009	1,363.00	1,072.90	290.10	21
White River Valley	Phreatophyte/Medium Density Vegetation	WRV2	2008	323.02	225.55	97.47	30

5.3   Limitations

The primary limitations that should be considered when evaluating the above results of the regression analysis include the quality and quantity of the basic data (i.e., Landsat TM 5 scenes and the annual ET data) and the data analysis performed. Because all Landsat scenes were acquired from one source (USGS EROS Data Center) and all ET data were acquired from agencies who used standardized methods to measure ET, any errors in these datasets should be systematic (i.e., the same throughout) rather than random. Therefore, the limitations discussed below focus on the quantity of data and the data analysis performed.

The quantity of Landsat data is dependent upon cloud-free or nearly cloud-free (less than 30 percent cloud cover) conditions during satellite acquisition. Four of the five years during this study period had sufficient cloud-free/low cloud-cover conditions throughout the growing season to provide enough Landsat images to adequately represent each month of the growing period. However, during the fifth year (2010) for White River Valley, there were limited cloud-free images available during the critical portion of the growing season, i.e., June and early July, and only one image (May 14) was available prior to the onset of summer heat and the associated decline in the amount of transpiring green vegetation. The lack of cloud-free imagery during the peak growing season for WRV in 2010 would likely result in a potential underestimate of ET for that year.

The quantity of ET data was impacted by the operational status of each EC station. During the growing season, when an EC station was non-functional or yielded data of insufficient quality due to sensor malfunction or adverse weather conditions, records were estimated. Additionally, records were missing due to sensor calibration which was typically performed during the period commensurate with the end and the start of the growing season. These periods were not estimated. The estimation methods are described in Section 3.0, and in more detail in Shanahan et al. (2011).

The calculation of vegetation indices, while providing a quantitative assessment of green vegetation, does not provide an assessment of soil water status and climate factors (e.g., air temperature, wind

speed, relative humidity) which control ET. As a consequence, there is never a direct one-to-one correspondence between ET and vegetation indices such as NDVI. However, as demonstrated by the analysis in this report and as discussed in Glenn et al. (2007), empirical relationships based on vegetation indices such as NDVI do provide a consistent and fairly accurate means of estimating total annual ET on an areal basis given the availability of measured ET for the area of interest.

This Page Left Intentionally Blank

6.0 SUMMARY AND CONCLUSIONS

This report documents the acquisition, processing, and analysis of micrometeorological data and satellite imagery collected as part of a multi-year collaborative investigation completed by UNLV, DRI, and SNWA to evaluate and quantify ET within groundwater discharge areas of White River, Spring and Snake Valleys, Nevada.

Ten ET-measurement sites were selected for monitoring within the groundwater discharge areas of the basins of interest. The site locations were selected to represent a range of uniform-composition phreatophytic vegetation for defined land-cover classifications. Of the 10 sites, one was located in White River Valley, seven in Spring Valley, and two in Snake Valley. At these sites, EC and meteorological stations were deployed to measure the energy fluxes and atmospheric conditions driving the ET process. These measurements were made during the period 2006 through 2010 by UNLV, DRI, and SNWA, and were collected, processed, and evaluated using standard methods based on the sensor manufacturer, Fluxnet-Canada, and Ameriflux guidelines. A total of 38 annual ET measurements were derived for these sites during the period of data collection.

Landsat TM 5 scenes were acquired for all cloud-free or nearly cloud-free image acquisition dates that encompassed the growing season for the five-year study period. Consistent methods were employed to radiometrically calibrate, atmospherically correct and normalize, and then calculate yearly average growing season NDVI grids from the Landsat scenes. Footprint analysis was performed using the EC- and meteorological-station data. The annual footprints were calculated to provide a quantitative assessment of the land areas around each station. The calculation method accounted for differences in contributions to the measured ET value by the land areas surrounding a given EC station, using weighing factors. The areas providing the largest contributions to measured ET would receive a larger weighting factor than areas contributing relatively little to the measured ET. The "footprint counts" were used as the weighing factors to calculate annual footprint-weighted average NDVI values.

Regression analysis was performed using SigmaPlot 11 statistical software and 31 data points comprised of annual ET and footprint-weighted average NDVI for the various ET-measurement sites and years. The remaining seven data points were reserved to perform an independent accuracy assessment of the regression-model predictions.

For the regression analysis, the annual ET values were set as the dependent variables and the corresponding footprint-weighted average NDVI values as the independent variables. Based on a review of the data, a linear-regression model was selected. The regression results indicated that a strong linear relationship exists between the two variables based on the resultant R-squared value of 0.953. The regression-model fit was assessed by evaluating the residuals between the measured and predicted annual ET values. An evaluation of the residuals indicated that the regression model does not have any significant biases and that the residuals are normally-distributed, reinforcing the

conclusion that a strong linear relationship exists between the two variables. The standard error of the estimate (σ_{est}) for the regression model was calculated as the square root of the sum of squared residuals divided by the number of data points (n=31) minus the degrees of freedom (df=1). The resultant value, 74.15 mm, is a measure of the accuracy of the prediction.

Seven data points were used in an independent accuracy assessment in which the predictive errors were calculated as the differences between the annual predicted ET minus the annual measured ET. For Spring Valley, the percent error ranged from 7 percent to 26 percent, with an average value of about 15 percent. For Snake and White River valleys, the percent errors were 32 percent and 30 percent, respectively.

Because the locations of the EC stations are representative of the vegetation and factors influencing ET across the broader expanse of the groundwater discharge areas of the basins of interest, the resulting annual ET should be a reasonably accurate estimate. During the initiation of the Devitt et al. (2008) and Arnone et al. (2008) studies, great care was taken in placing the EC stations in areas representing various vegetation and moisture conditions. In addition, standardized data analysis methods have been employed to process the data. Therefore, it is concluded here that the annual ET measurements are indeed representative of the broader landscape and that the resulting empirical relationship provides a scientifically sound basis for estimating annual ET for the groundwater discharge areas of White River, Spring, and Snake Valleys as presented in Burns and Drici (2011).

7.0 REFERENCES

Allen, R.G., Tasumi, M., Morse, A., and Trezza, R., 2005, A Landsat-based energy balance and evapotranspiration model in Western US water rights regulation and planning: Irrigation and Drainage Systems, Vol. 19, p. 251-268.

Allen, R.G., Tasumi, M., Morse, A., Trezza, R., Wright, J.L., Bastiaanssen, W., Kramber, W., Lorite, I., and Robison, C.W., 2007, Satellite-based energy balance for mapping evapotranspiration with internalized calibration (METRIC)–Applications: Journal of Irrigation and Drainage Engineering, Vol. 133, No. 4, p. 395-406.

Arnone, III, J.A., Jasoni, R.L., Larsen, J.D., Fenstermaker, L.F., Wohlfahrt, G., Kratt, C.B., Lyles, B.F., Healey, J., Young, M.H., and Thomas, J.M., 2008, Variable evapotranspirative water losses from lowland agricultural and native shrubland ecosystems in the eastern Great Basin of Nevada, USA: Desert Research Institute, Reno, Nevada, 97 p.

Baldocchi, D., Valentini, R., Running, S., Oechel, W., and Dahlman, R., 1996, Strategies for measuring and modelling carbon dioxide and water vapour fluxes over terrestrial ecosystems: Global Change Biology, Vol. 2, p. 159-168.

Bastiaanssen, W.G.M., Menenti, M., Feddes, R.A., and Holtslag, A.A.M., 1998a, A remote sensing surface energy balance algorithm for land (SEBAL) 1. Formulation: Journal of Hydrology, Vol. 212-213, p. 198-212.

Bastiaanssen, W.G.M., Pelgrum, H., Wang, J., Ma, Y., Moreno, J.F., Roerink, G.J., and van der Wal, T., 1998b, A remote sensing surface energy balance algorithm for land (SEBAL) 2. Validation: Journal of Hydrology, Vol. 212-213, p. 213-229.

Brustaert, W., 1982, Evaporation into the atmosphere: Theory, history, and applications. First edition: Dordrecht, The Netherlands, Kluwer Academic Publishers.

Burba, G., and Anderson, D., 2010, A brief practical guide to eddy covariance flux measurements: Principles and workflow examples for scientific and industrial applications. Lincoln, Nebraska, LI-COR Biosciences.

Burns, A.G., and Drici, W., 2011, Hydrology and water resources of Spring, Cave, Dry Lake, and Delamar valleys, Nevada and vicinity: Presentation to the Office of the Nevada State Engineer: Southern Nevada Water Authority, Las Vegas, Nevada.

Chander, G., Markham, B.L., and Helder, D., 2009, Summary of current radiometric calibration coefficients for Landsat MSS, TM, ETM+, and EO-1 ALI sensors: Remote Sensing of Environment, Vol. 113, p. 893-903.

Courault, D., Seguin, B., and Olioso, A., 2005, Review on estimation of evapotranspiration from remote sensing data: From empirical to numerical modeling approaches: Irrigation and Drainage Systems, Vol. 19, p. 223-249.

Devitt, D., Fenstermaker, L., Young, M., Conrad, B., Baghzouz, M., and Bird, B., 2008, Evapotranspiration estimates in north eastern Nevada basins: University of Nevada, Las Vegas, 256 p.

Devitt, D.A., Fenstermaker, L.F., Young, M.H., Conrad, B., Baghzouz, M., and Bird, B.M., 2010, Evapotranspiration of mixed shrub communities in phreatophytic zones of the Great Basin region of Nevada (USA). Ecohydrology, 4:n/a. doi: 10.1002/eco.169.

EdiRe, 1999, Eddy covariance software package, Version 1.5.0.10 [Internet], [accessed September 7, 2010], available from http://www.geos.ed.ac.uk/abs/research/micromet/EdiRe/Downloads.html.

Falge, E., Baldocchi, D., Olson, R., Anthoni, P., Aubinet, M., Bernhofer, C., Burba, G., Ceulemans, R., Clement, R., Dolman, H., et al., 2001, Gap filling strategies for long term energy flux data sets: Agricultural and Forest Meteorology, Vol. 107, p. 71-77.

Farrand, W.H., Singer, R.B., and Merényi, E., 1994, Retrieval of apparent surface reflectance from AVIRIS data: A comparison of empirical line, radiative transfer, and spectral mixture methods: Remote Sensing of Environment, Vol. 47, p. 311-321.

Fluxnet-Canada Network Management Office, 2003, Fluxnet-Canada measurement protocols: Working draft-Version 1.3 [Internet], [accessed March 24, 2008], available from http://www.fluxnet-canada.ca/pages/protocols_en/measurement%20protocols_v.1.3_background .pdf.

Foken, T., 2008, The energy balance closure problem: An overview: Ecological Applications, Vol. 18, No. 6, p. 1351-1367.

Foken, T., and Wichura, B., 1996, Tools for quality assessment of surface-based flux measurements: Agricultural and Forest Meteorology, Vol. 78, p. 83-105.

Foken, T., Göckede, M., Mauder, M., Mahrt, L., Amiro, B., and Munger, W., 2004, Post-field data quality control, *in* Lee, X., Massman, W.J., and Law, B., eds., Handbook of Micrometeorology: A guide for surface flux measurement and analysis. Dordrecht, The Netherlands, Kluwer Academic Press, p. 181-208.

Foken, T., Wimmer, F., Mauder, M., Thomas, C., and Liebethal, C., 2006, Some aspects of the energy balance closure problem: Atmospheric Chemistry and Physics Discussions, Vol. 6, p. 3381-3402.

Gao, Y., and Long, D., 2008, Intercomparison of remote sensing-based models for estimation of evapotranspiration and accuracy assessment based on SWAT: Hydrological Processes, Vol. 22, p. 4850-4869.

Glenn, Edward P., Huete, Alfredo R., Nagler, Pamela L., Hirschboeck, Katherine K., and Brown, Paul (2007) "Integrating Remote Sensing and Ground Methods to Estimate Evapotranspiration," Critical Reviews in Plant Sciences, 26:3, 139-168.

Groeneveld, D.P., Baugh, W.M., Sanderson, J.S., and Cooper, J.S., 2007, Annual groundwater evapotranspiration mapped from single satellite scenes: Journal of Hydrology, Vol. 344, p. 146-156.

Højstrup, J., 1993, A statistical data screening procedure: Measurement Science and Technology, Vol. 4, p. 153-157.

Hong, S., 2008, Mapping regional distributions of energy balance components using optical remotely sensed imagery [Ph.D. dissertation]: New Mexico Institute of Mining and Technology Department of Earth and Environmental Science, Socorro, New Mexico, 378 p.

Hsieh, C., Katul, G., and Chi, T., 2000, An approximate analytical model for footprint estimation of scalar fluxes in thermally stratified atmospheric flows: Advances in Water Resources, Vol. 23, p. 765-772.

Huete, A., Didan, K., Miura, T., Rodriguez, E.P., Gao, X., and Ferreira, L.G., 2002, Overview of the radiometric and biophysical performance of the MODIS vegetation indices: Remote Sensing of Environment, Vol. 83, p. 195–213.

Huntington, J.L., and Allen, R.G., 2010, Evapotranspiration and net irrigation water requirements for Nevada: Department of Conservation and Natural Resources–Division of Water Planning, Carson City, Nevada, 288 p.

Kohsiek, W., Liebethal, C., Foken, T., Vogt, R., Oncley, S.P., Bernhofer, C., and de Bruin, H.A.R., 2007, The energy balance experiment EBEX-2000. Part III: Behaviour and quality of the radiation measurements: Boundary-Layer Meteorology, Vol. 123, No. 1, p. 55-75.

Kustas, W.P., Perry, E.M., Doraiswamy, P.C., and Moran, M.S., 1994, Using satellite remote sensing to extrapolate evapotranspiration estimates in time and space over a semiarid rangeland basin: Remote Sensing of Environment, Vol. 49, p. 275-286.

Lee, X., Massman, W., and Law, B., eds., 2004, Handbook of Micrometeorology: A guide for surface flux measurement and analysis. Dordrecht, The Netherlands, Kluwer Academic Press.

Liu, H., Peters, G., and Foken, T., 2001, New equations for sonic temperature variance and buoyancy heat flux with an omnidirectional sonic anemometer: Boundary-Layer Meteorology, Vol. 100, p. 459-468.

Massman, W.J., 2000, A simple method for estimating frequency response corrections for eddy covariance systems: Agricultural and Forest Meteorology, Vol. 104, p. 185-198.

Massman, W.J., 2001, Reply to comment by Rannik on "A simple method for estimating frequency response corrections for eddy covariance systems": Agricultural and Forest Meteorology, Vol. 107, p. 247-251.

Massman, W.J., and Lee, X., 2002, Eddy covariance flux corrections and uncertainties in long-term studies of carbon and energy exchanges: Agricultural and Forest Meteorology, Vol. 113, p. 121-144.

Mauder, M., Oncley, S.P., Vogt, R., Weidinger, T., Ribeiro, L., Bernhofer, C., Foken, T., Kohsiek, W., de Bruin, H.A.R., and Liu, H., 2007, The energy balance experiment EBEX-2000. Part II: Intercomparison of eddy-covariance sensors and post-field data processing methods: Boundary-Layer Meteorology, Vol. 123, No. 1, p. 29-54.

Moran, M.S., and Jackson, R.D., 1991, Assessing the spatial distribution of evapotranspiration using remotely sensed inputs: Journal of Environmental Quality, Vol. 20, No. 4, p. 725-737.

Moreo, M.T., Laczniak, R.J., and Stannard, D.I., 2007, Evapotranspiration rate measurements of vegetation typical of ground-water discharge areas in the Basin and Range carbonate-rock aquifer system, Nevada and Utah, September 2005–August 2006: U.S. Geological Survey Scientific-Investigations Report 2007-5078, 36 p.

Munger, J.W., and Loescher, H.W., 2006, Guidelines for making eddy covariance flux measurements [Internet], [accessed February 28, 2011], available from http://public.ornl.gov/ameriflux/sop.shtml.

Nagler, P.L., 2009, Personal communication of September 2009 to R. Shanahan (Southern Nevada Water Authority) regarding Technical Reviews of Arnone et al. 2008 and Devitt et al. 2008 reports: U.S. Geological Survey.

Nagler, P.L., Glenn, E.P., Kim, H., Emmerich, W., Scott, R.L., Huxman, T.E., and Huete, A.R., 2007, Relationship between evapotranspiration and precipitation pulses in a semiarid rangeland estimated by moisture flux towers and MODIS vegetation indices: Journal of Arid Environments, Vol. 70, p. 443-462.

Nagler, P.L., Scott, R.L., Westenburg, C., Cleverly, J.R., Glenn, E.P., and Huete, A.R., 2005, Evapotranspiration on western U.S. rivers estimated using the Enhanced Vegetation Index from MODIS and data from eddy covariance and Bowen ratio flux towers: Remote Sensing of Environment, Vol. 97, p. 337-351.

Nichols, W.D., 2000, Regional ground-water evapotranspiration and ground-water budgets, Great Basin, Nevada: U.S. Geological Survey Professional Paper 1628, 101 p.

Oke, T.R., 1987, Boundary layer climates. Second edition: New York, Routledge Taylor & Francis Group.

Oncley, S.P, Foken, T., Vogt, R., Kohsiek, W., de Bruin, H.A.R., Bernhofer, C., Christen, A., van Gorsel, E., Grantz, D., Feigenwinter, C., et al., 2007, The energy balance experiment EBEX-2000. Part I: Overview and energy balance: Boundary-Layer Meteorology, Vol. 123, No. 1, p. 1-28.

Reichstein, M., 2008, Personal communication of September 10 to B. Bird (Southern Nevada Water Authority) regarding the implementation of the online-tool for U*-filtering and gap-filling of eddy flux data: Max-Planck Institute for Biogeochemistry, Jena, Germany.

Reichstein, M., Falge, E., Baldocchi, D., Papale, D., Aubinet, M., Berbigier, P., Bernhofer, C., Buchmann, N., Gilmanov, T., Granier, A., et al., 2005, On the separation of net ecosystem exchange into assimilation and ecosystem respiration: Review and improved algorithm: Global Change Biology, Vol. 11, p. 1424-1439.

Rouse, Jr., J.W., Haas, R.H., Schell, J.A., and Deering, D.W., 1974, Monitoring vegetation systems in the Great Plains with ERTS: Proceedings of the Third Earth Resources Technology Satellite-1 Symposium, Paper A20, p. 301-317.

Running, S.W., and Nemani, R.R., 1988, Relating seasonal patterns of the AVHRR vegetation index to simulated photosynthesis and transpiration of forests in different climates: Remote Sensing of Environment, Vol. 24, p. 347-367.

Sajwaj, T., 2003, Field Methodologies and Training Manual for Nevada Field Crews: Southwest Regional Gap Analysis Project (SW ReGAP): U.S. Environmental Protection Agency, 70 p.

Schotanus, P., Nieuwstadt, F.T.M., and de Bruin, H.A.R., 1983, Temperature measurement with a sonic anemometer and its application to heat and moisture fluxes: Boundary-Layer Meteorology, Vol. 26, p. 81-93.

Shanahan, R.D., Collins, C.A., and Burns, A.G, 2011, 2006-2010 Evapotranspiration Data Report: Southern Nevada Water Authority, Las Vegas, Nevada, Doc. No. HAM-ED-0003, 81 p.

Smith, G.M., and Milton, E.J., 1999, The use of empirical line method to calibrate remotely sensed data to reflectance: International Journal of Remote Sensing, Vol. 20, No. 13, p. 2653-2662.

Smith, J.L., Laczniak, R.J., Moreo, M.T., and Welborn, T.L., 2007, Mapping evapotranspiration units in the Basin and Range carbonate-rock aquifer system, White Pine County, Nevada, and adjacent areas in Nevada and Utah: U.S. Geological Survey Scientific Investigations Report 2007-5087, 20 p.

Szilagyi, J., 2000, Can a vegetation index derived from remote sensing be indicative of areal transpiration?: Ecological Modelling, Vol. 127, p. 65-79.

Szilagyi, J., 2002, Vegetation indices to aid areal evapotranspiration estimations: Journal of Hydrologic Engineering, Vol. 7, p. 368-372.

Tucker, C.J., 1979, Red and photographic infrared linear combinations for monitoring vegetation: Remote Sensing of Environment, Vol. 8, p. 127-150.

Tuya, S., Batjargal, Z., Kajiwara, K., and Honda, Y. (2005) Satellite-derived estimates of evapotranspiration in the arid and semi-arid region of Mongoliá, International Journal of Environmental Studies, 62:5, 517-526.

Vickers, D., and Mahrt, L., 1997, Quality control and flux sampling problems for tower and aircraft data: Journal of Atmospheric and Oceanic Technology, Vol. 14, p. 512-526.

Webb, E.K., Pearman, G.I., and Leuning, R., 1980, Correction of flux measurements for density effects due to heat and water vapour transfer: Quarterly Journal of Royal Meteorology Society, Vol. 106, p. 85-100.

Welch, A.H., Bright, D.J., and Knochenmus, L.A., eds., 2007, Water resources of the Basin and Range carbonate-rock aquifer system, White Pine County, Nevada, and adjacent areas in Nevada and Utah: U.S. Geological Survey Scientific Investigations Report 2007-5261, 96 p.

Wilczak, J.M., Oncley, S.P., and Stage, S.A., 2001, Sonic anemometer tilt correction algorithms: Boundary-Layer Meteorology, Vol. 99, p. 127-150.

Wilson, K.B., et al., Energy partitioning between latent and sensible heat flux during the warm season at FLUXNET sites, *Water Resour. Res.*, 38(12), 1294, doi:10.1029/2001WR00989, 2002.

Wohlfahrt, G., Fenstermaker, L.F., and Arnone, III, J.A., 2008, Large annual net ecosystem CO_2 uptake of a Mojave Desert ecosystem: Global Change Biology, Vol. 14, p. 1-13.

Wohlfahrt, G., Haslwanter, A., Hörtnagl, L., Jasoni, R.L., Fenstermaker, L.F., Arnone III, J.A., and Hammerle, A., 2009, On the consequences of the energy imbalance for calculating surface conductance to water vapour: Agricultural and Forest Meteorology, Vol. 149, p. 1556-1559.

Xu, L., 2004, Processing notes for the open-path "Gold" file [Internet], [accessed February 28, 2011], available from http://cdiac.esd.ornl.gov/ftp/ameriflux/gold/Open_Path/Gold_processing_openpath_notes_0410.doc.

Zhu, J., Young, M.H., and Cablk, M.E., 2007, Uncertainty analysis of estimates of ground-water discharge by evapotranspiration for the BARCAS study area: Desert Research Institute Las Vegas, Nevada, Publication No. 41234, 36 p.
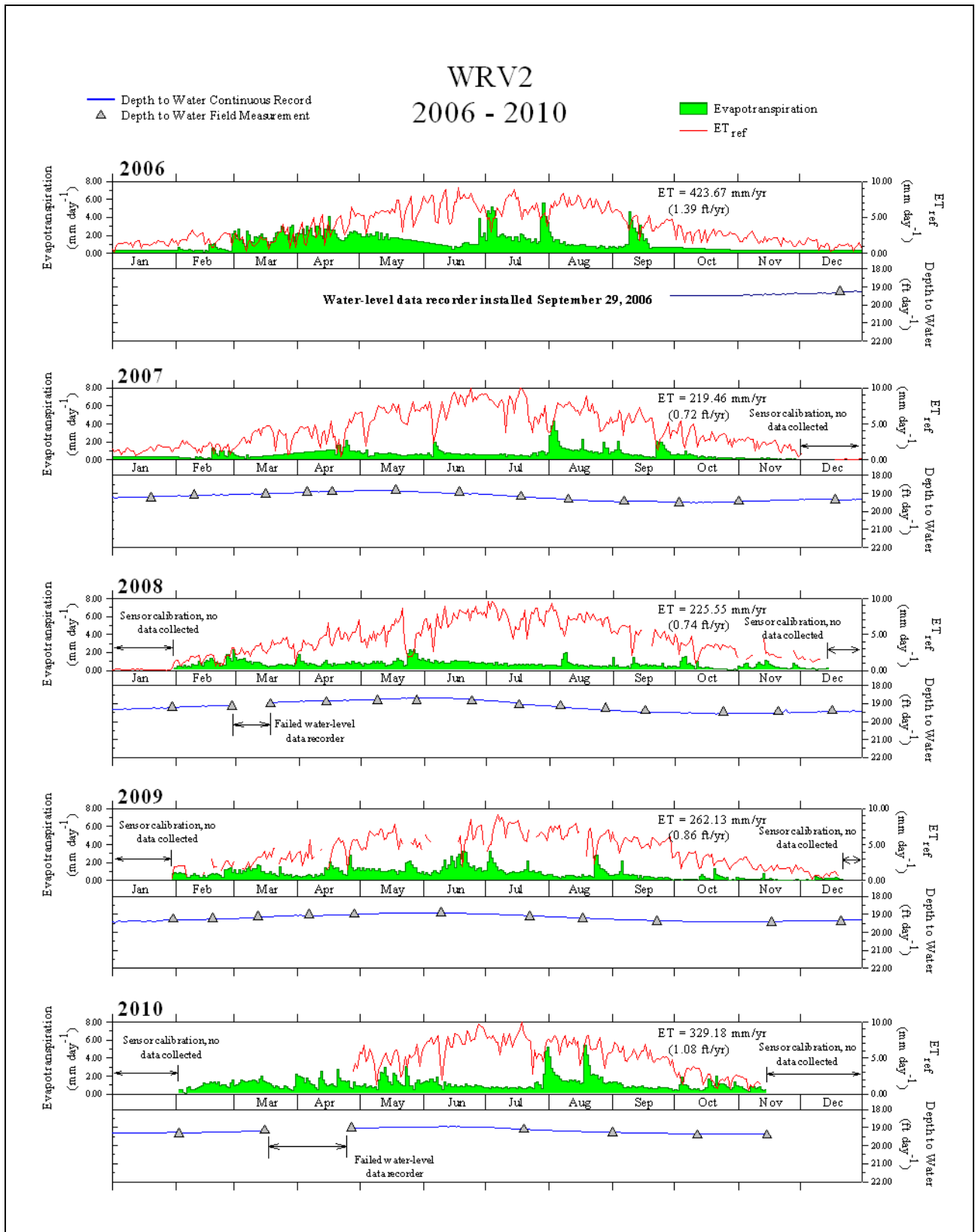
Appendix A

ET-Station Data

Figure A-1
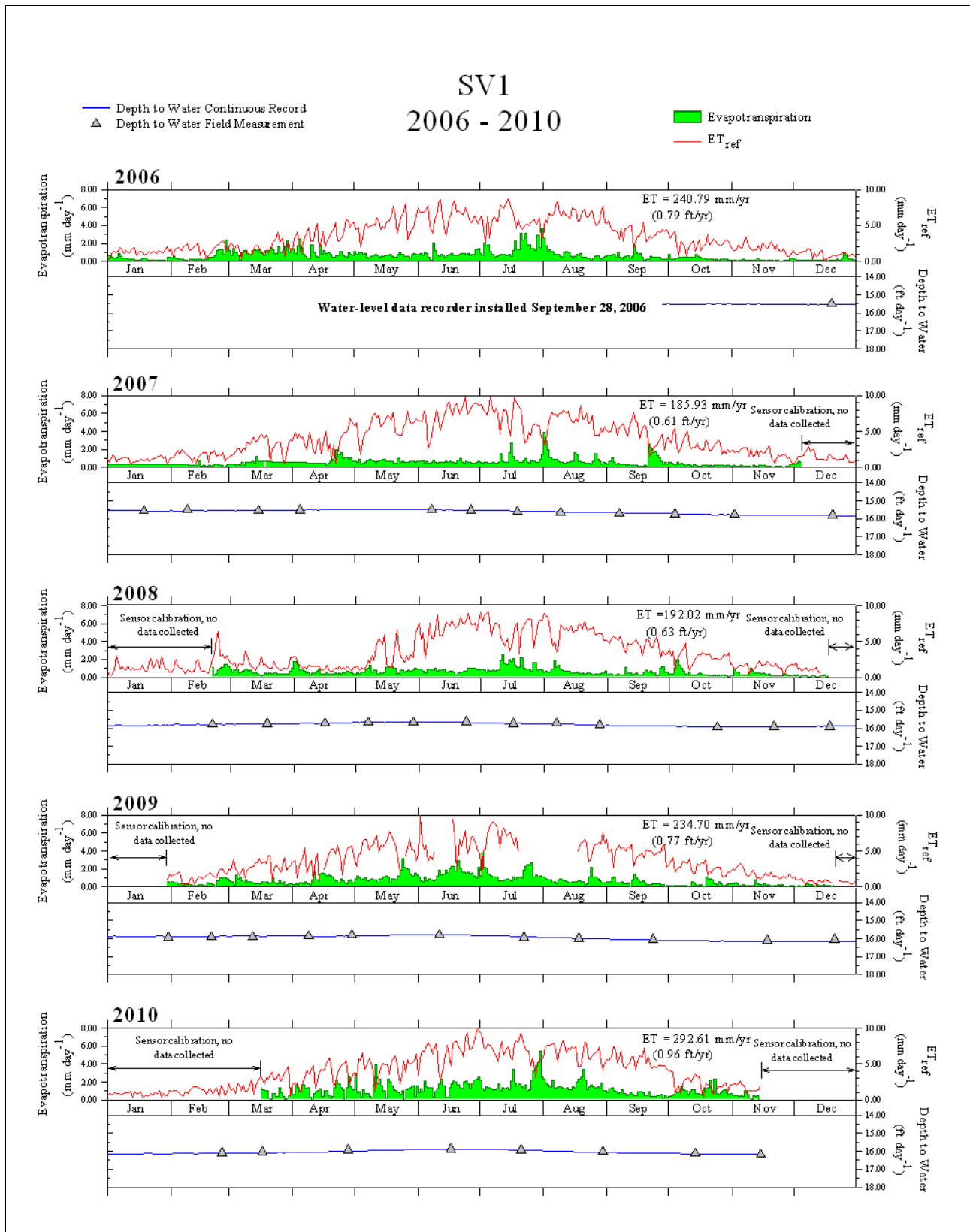**Daily ET, ET_ref and Depth-to-Water at WRV2 2006-2010**

Figure A-2
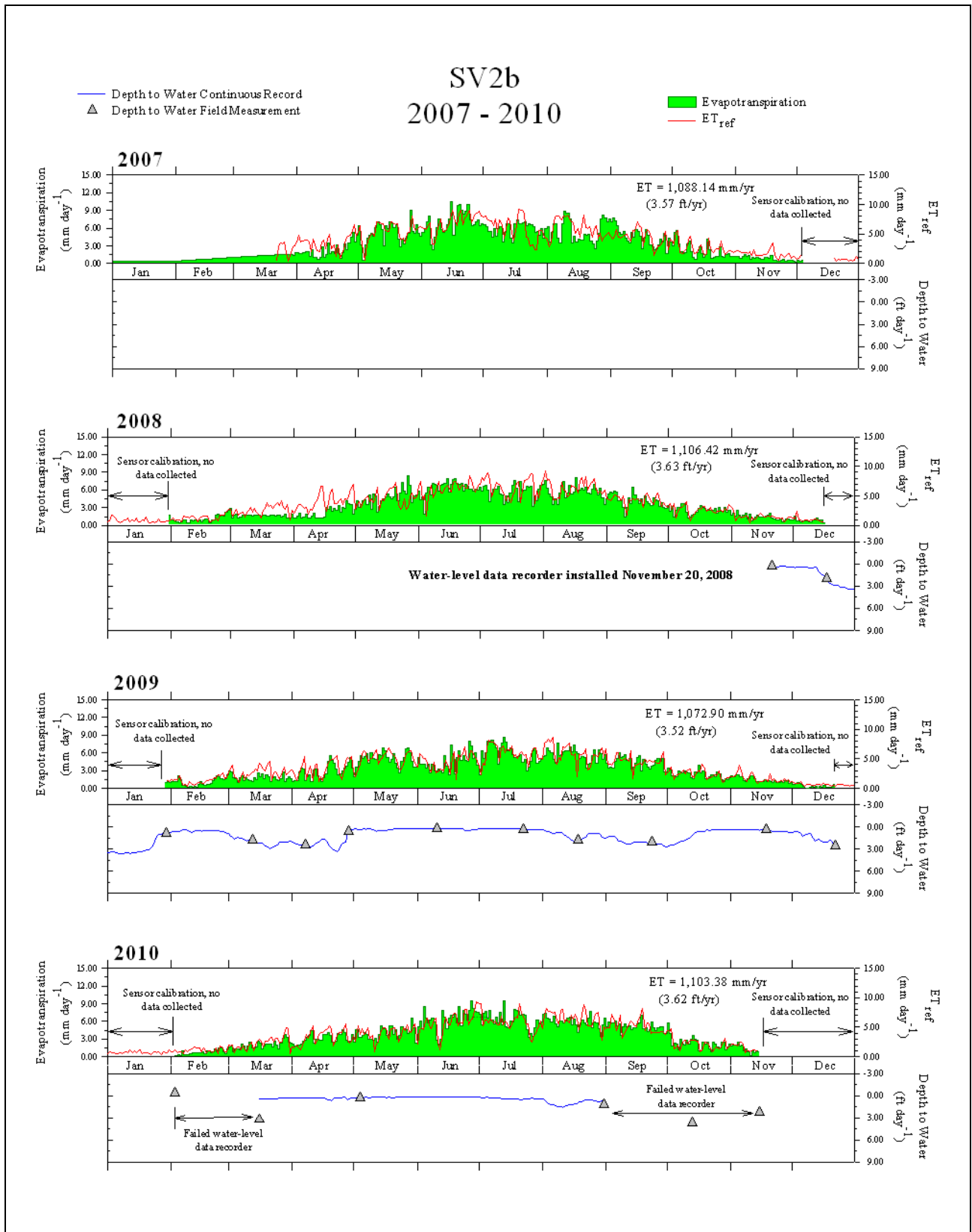**Daily ET, ET$_{ref}$ and Depth-to-Water at SV1 2006-2010**

Figure A-3
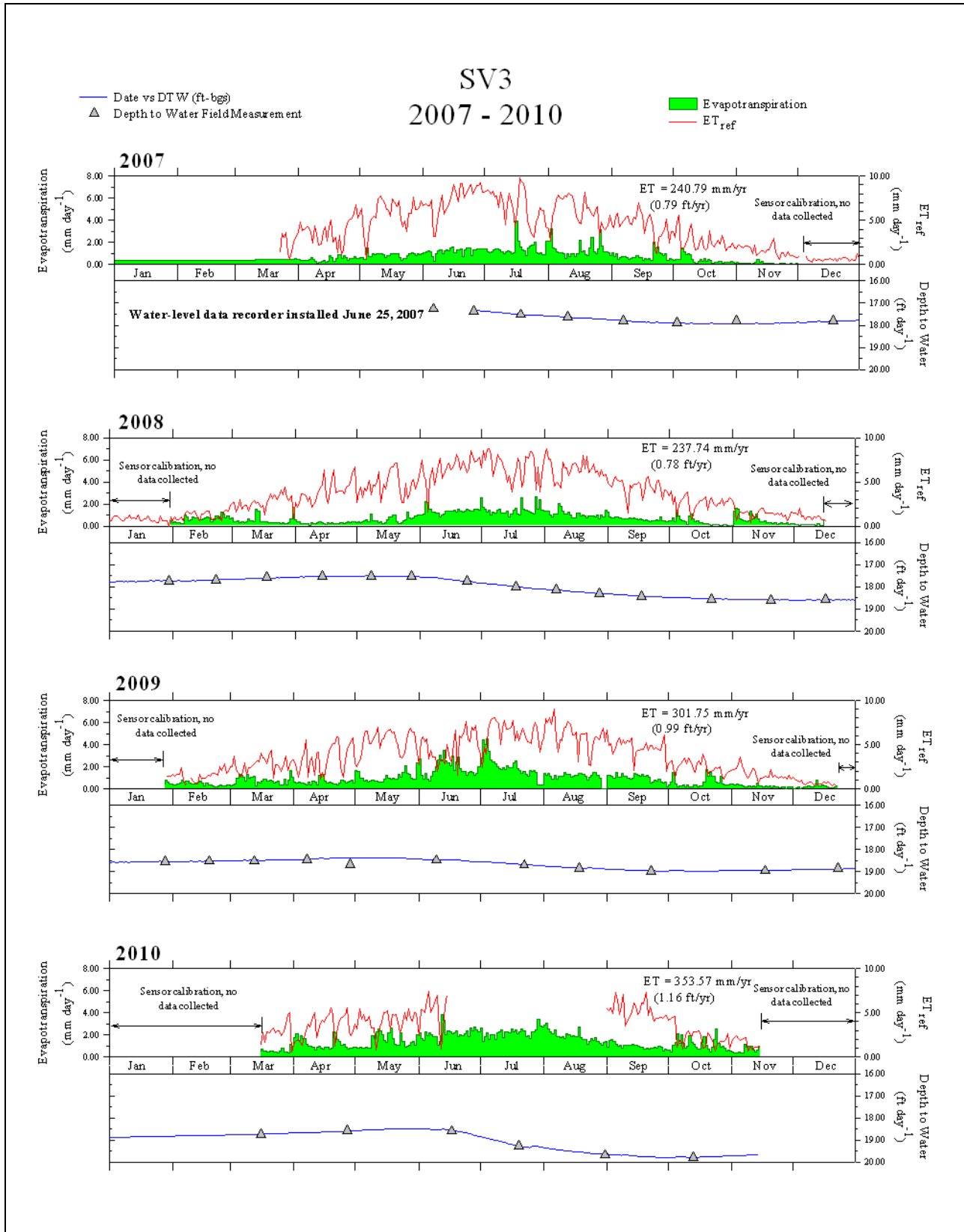**Daily ET, ET_ref and Depth-to-Water at SV2b 2007-2010**

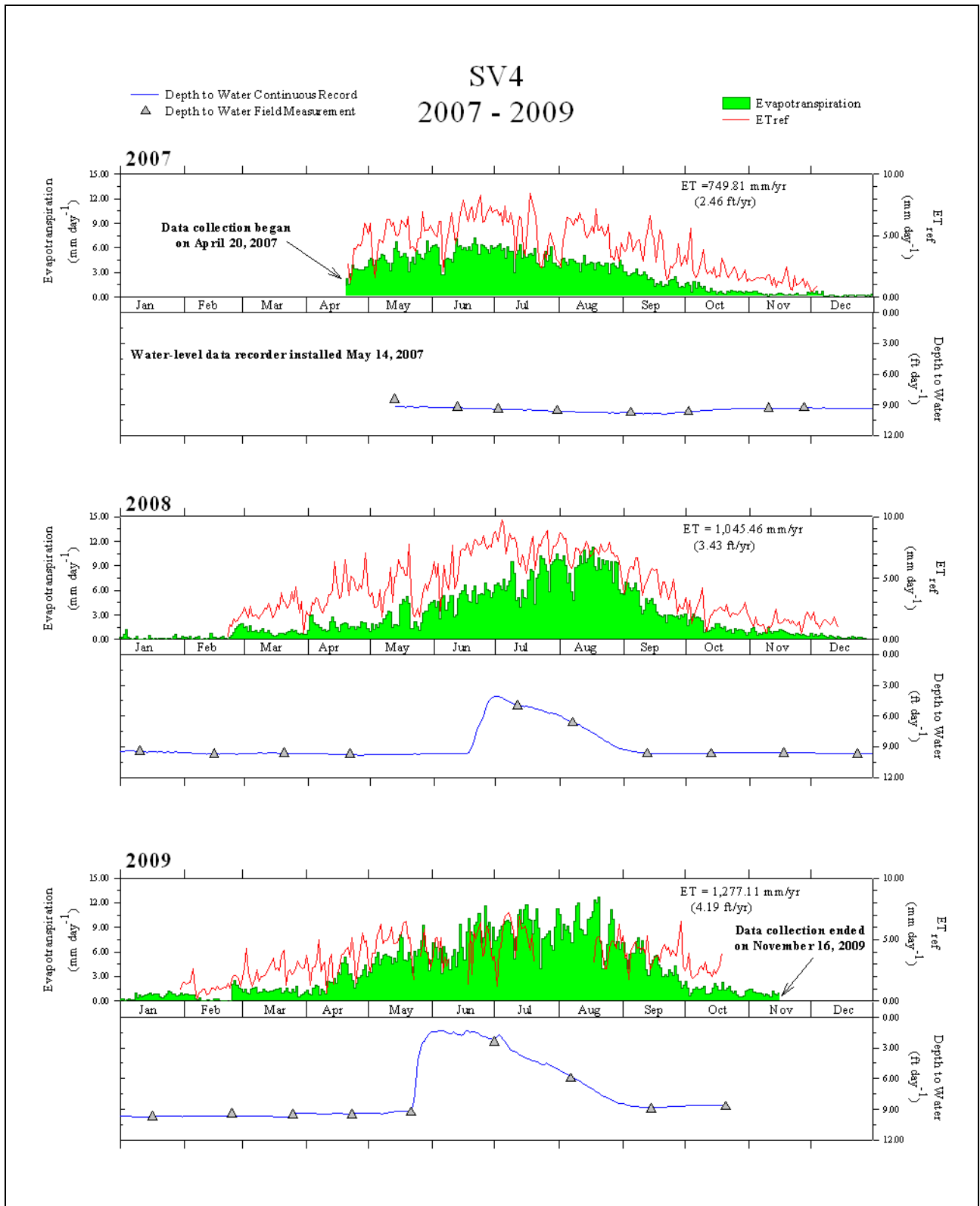**Figure A-4**
Daily ET, ET_ref and Depth-to-Water at SV3 2007-2010

Figure A-5
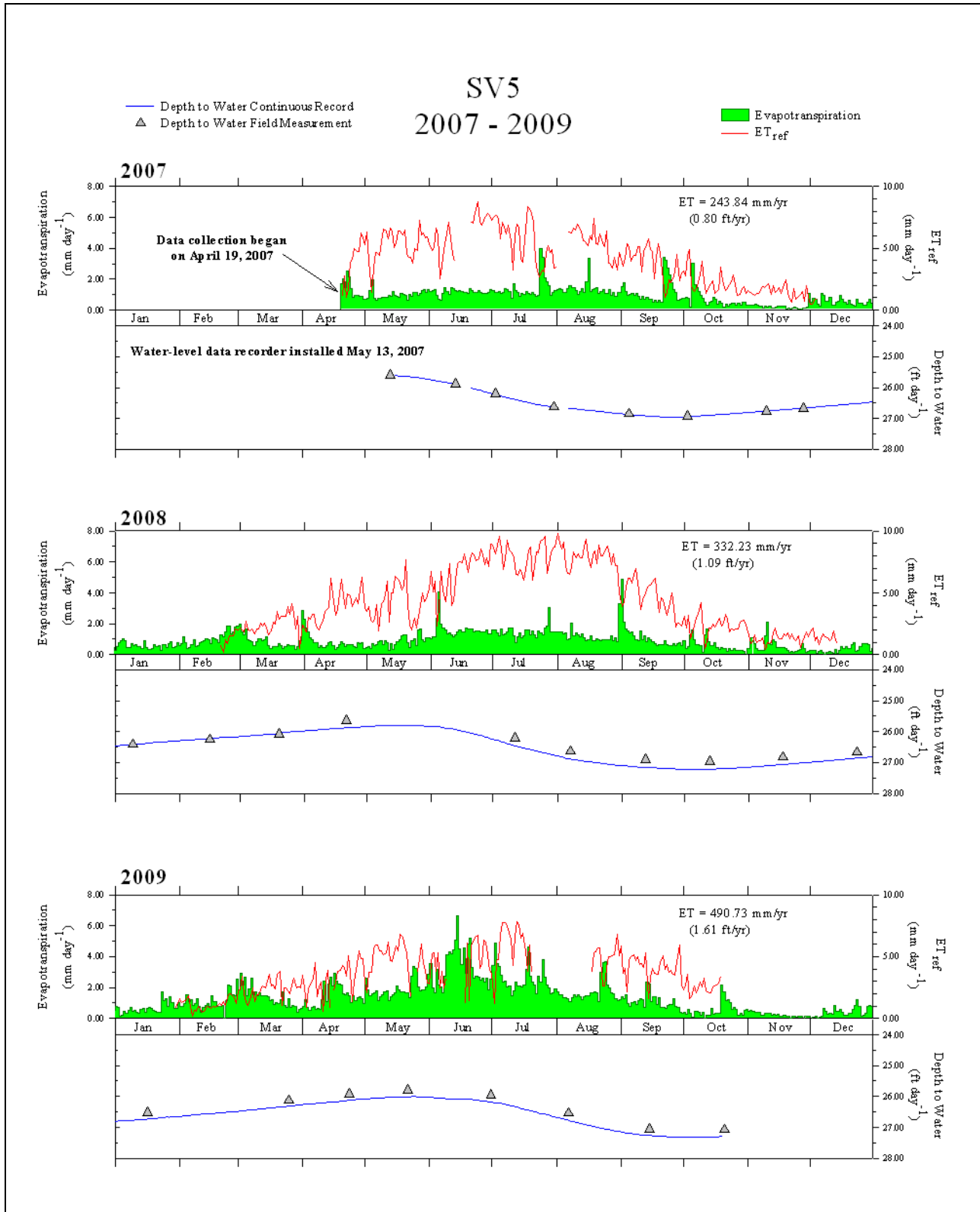**Daily ET, ET$_{ref}$ and Depth-to-Water at SV4 2007-2009**

Figure A-6
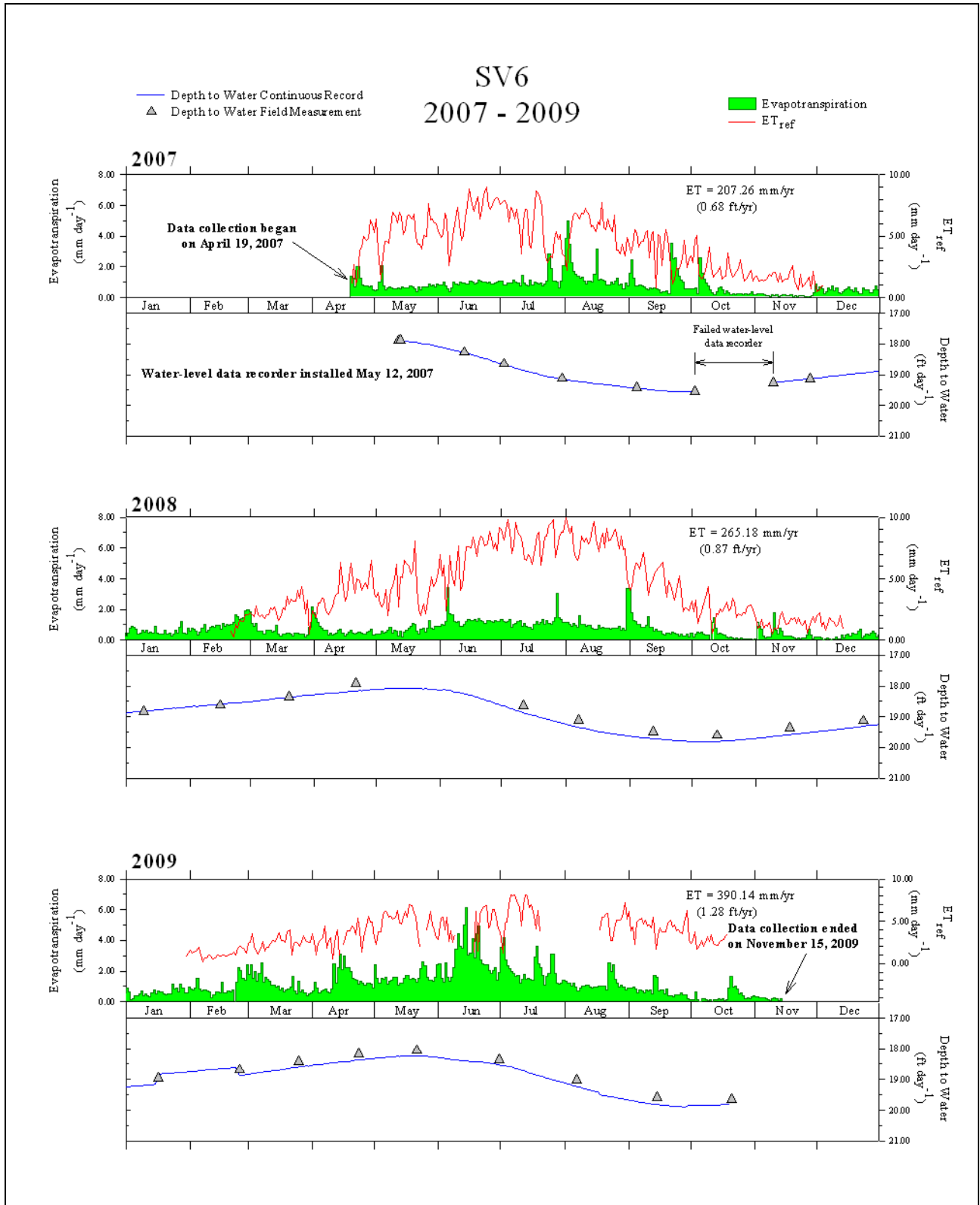**Daily ET, ET$_{ref}$ and Depth-to-Water at SV5 2007-2009**

Figure A-7
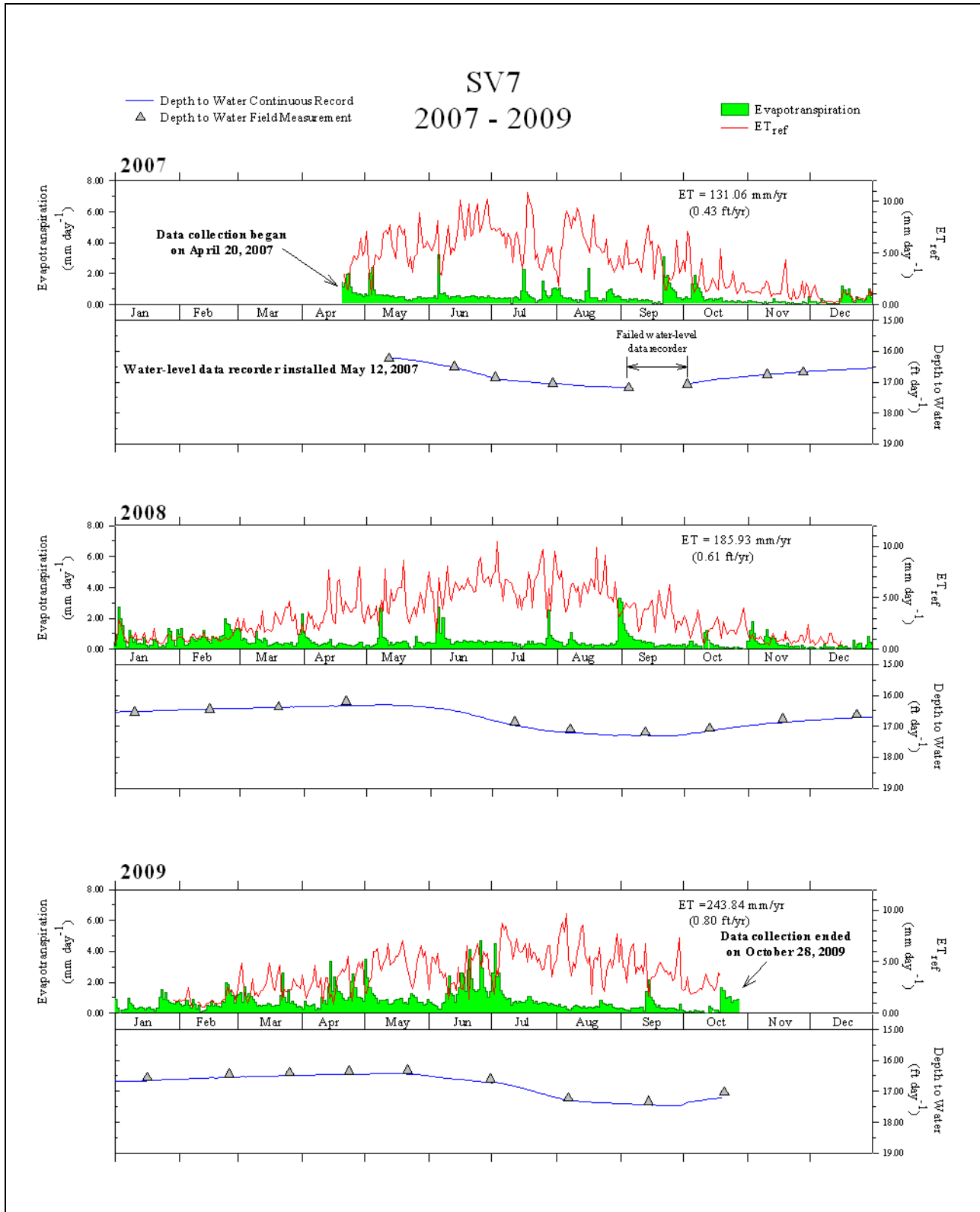**Daily ET, ET$_{ref}$ and Depth-to-Water at SV6 2007-2009**

Figure A-8
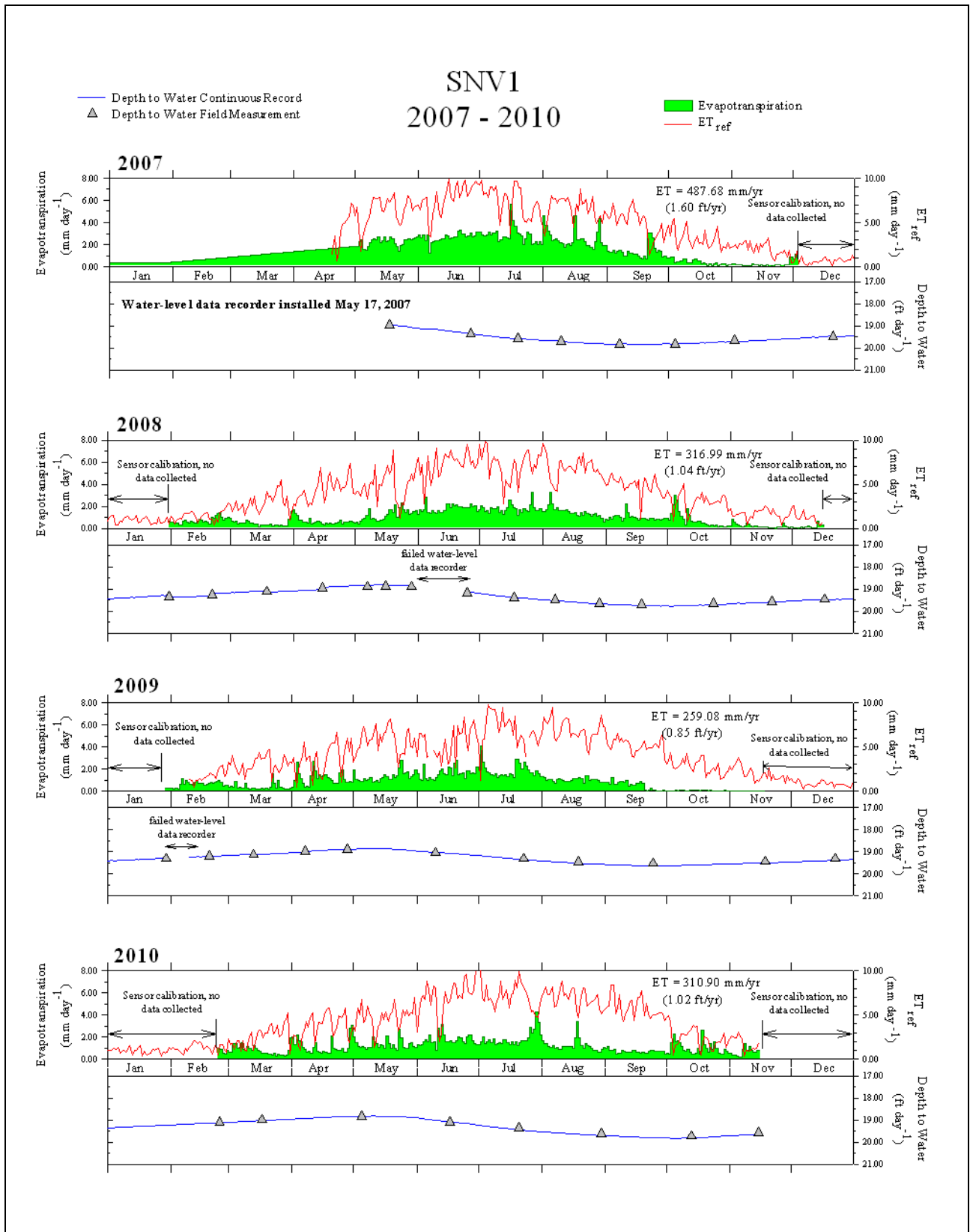**Daily ET, ET$_{ref}$ and Depth-to-Water at SV7 2007-2009**

Figure A-9
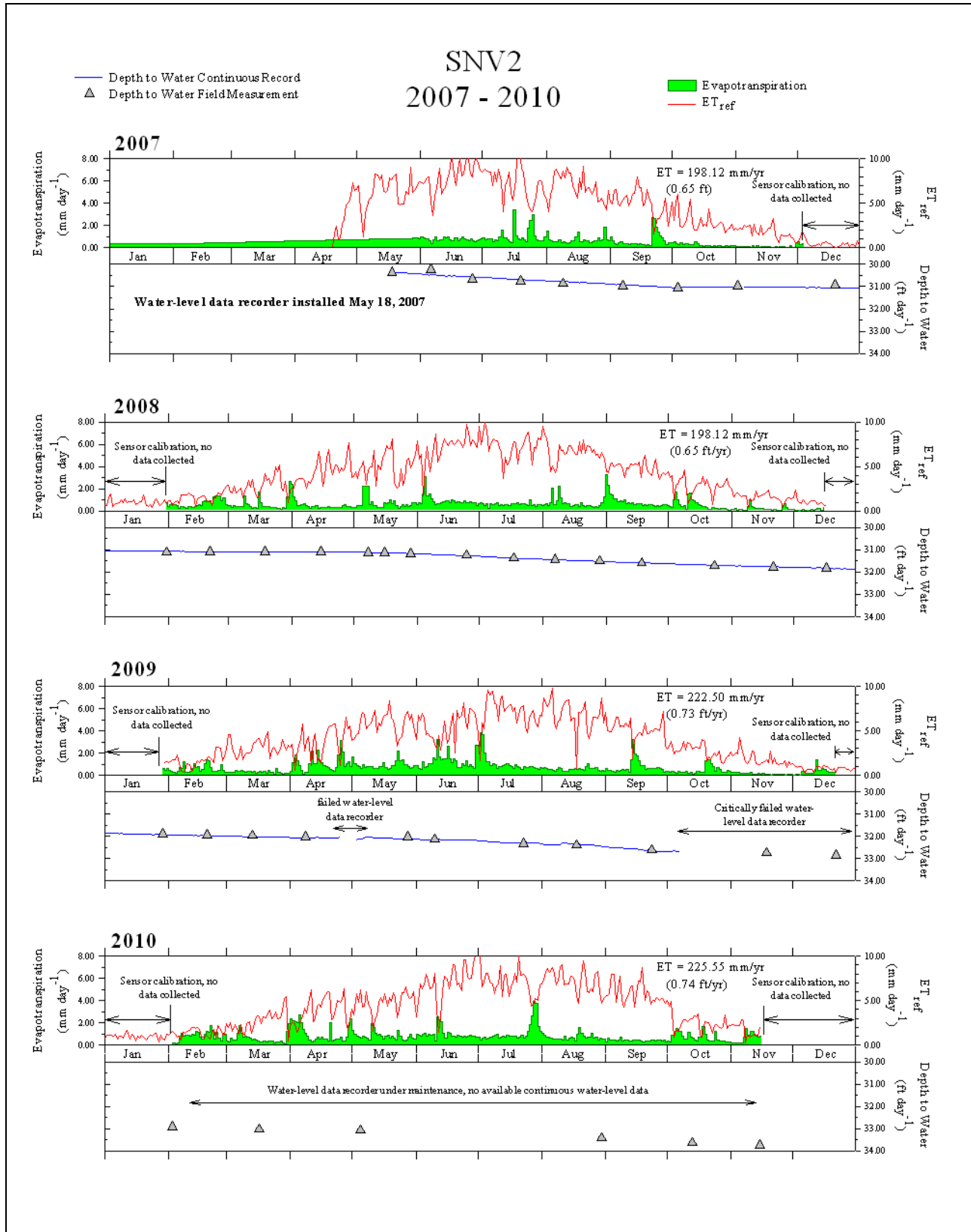**Daily ET, ET_{ref} and Depth-to-Water at SNV1 2007-2010**

Figure A-10
Daily ET, ET$_{ref}$ and Depth-to-Water at SNV2 2007-2010

Table A-1
Annual ET (ft)

Site Name	2006	2007	2008	2009	2010	Period of Record[d]
WRV2	1.39[a]	0.72[b]	0.74	0.86	1.08	January 2006 - November 2010
SV1	0.79[a]	0.61[b]	0.63	0.77	0.96	January 2006 - November 2010
SV2b	---	3.57[b]	3.63	3.52	3.62	March 2007 - November 2010
SV3	---	0.79[b]	0.78	0.99	1.16	March 2007 - November 2010
SV4	---	2.46[c]	3.43[c]	4.19[c]	---	April 2007 - November 2009
SV5	---	0.80[c]	1.09[c]	1.61[c]	---	April 2007 - December 2009
SV6	---	0.68[c]	0.87[c]	1.28[c]	---	April 2007 - November 2009
SV7	---	0.43[c]	0.61[c]	0.80[c]	---	April 2007 - October 2009
SnV1	---	1.60[b]	1.04	0.85	1.02	May 2007 - November 2010
SnV2	---	0.65[b]	0.65	0.73	0.74	May 2007 - November 2010

Note: All annuals are January through December.
[a]Devitt et al. (2008, p. 40).
[b]These include additional data not reported in Devitt et al. (2008).
[c]Data collected by DRI personnel and processed by SNWA.
[d]Sites were not operational during periods of sensor calibration (typically late December through middle February).

References

Devitt, D., Fenstermaker, L., Young, M., Conrad, B., Baghzouz, M., and Bird, B., 2008, Evapotranspiration estimates in north eastern Nevada basins: University of Nevada, Las Vegas, 256 p.